FOURIER PTYCHOGRAPHY MICROSCOPY – PORTABILITY AND COMPUTATION PROBED BY POINT OF CARE ANALYSIS

A THESIS SUBMITTED TO

THE FACULTY OF ACHITECTURE AND ENGINEERING

OF

EPOKA UNIVERSITY

BY

GENT IMERAJ

IN PARTIAL FULFILLMENT OF THE REQUIREMENTS
FOR
THE DEGREE OF MASTER OF SCIENCE
IN
ELECTRONICS AND COMMUNICATION ENGINEERING

MONTH (JULY), Year (2021)

Approval sheet of the Thesis

This is to certify that we have read this thesis entitled **"**Fourier Ptychography Microscopy – Portability and Computation Probed by Point of Care Analysis" and that in our opinion it is fully adequate, in scope and quality, as a thesis for the degree of Master.

_____

Assist. Prof. Dr. Arban UKA
Head of Department
Date: __/__/____

Examining Committee Members:

Dr. M. Maaruf Ali	(Computer Engineering)	_____
Assoc.Prof.Dr. Carlo Ciulla	(Computer Engineering)	_____
Assist. Prof. Dr. Arban UKA	(Computer Engineering)	_____

I hereby declare that all information in this document has been obtained and presented in accordance with academic rules and ethical conduct. I also declare that, as required by these rules and conduct, I have fully cited and referenced all material and results that are not original to this work.

Name, Last name: Gent, IMERAJ

Signature:

ABSTRACT

FOURIER PTYCHOGRAPHY MICROSCOPY – PORTABILITY AND COMPUTATION PROBED BY POINT OF CARE ANALYSIS

IMERAJ, Gent

M.Sc., Department of Computer Engineering

Supervisor: Assist. Prof. Dr. Arban UKA

Medical imaging is a growing field that has stemmed from the need to conduct non-invasive diagnosis, monitoring and analysis of biological systems. We focused on image acquisition and image analysis using portable microscopes for point-of-care (POC) analysis and image analysis on portable computing units. This thesis focuses on Fourier ptychography, by drawing the experience from Digital In Line Holography and Bright Field Microscopy, previously concluded in other thesis of the author. FP is a computational imaging technique which makes use of a matrix illumination to acquire a set of low-resolution images, that are used to reconstruct a complex image, resulting in a high space-bandwidth product. There are 3 hypotheses in this theses that have been verified / upgraded regarding FP improvement from experimental methodology and theoretical approach. It is proved that by manually focusing the images for a 5x5 dataset to be used in FP, the result complex output has an increased resolution. Also, by changing the wavelength of the LED light source when acquiring the dataset, it produces a different output image. Since smaller wavelength is higher frequency, and high frequency is resolution in k-space, the output image should be of better quality for small wavelengths (green or blue). The third component has observed the bandwidth of the light source itself, by replacing LED light with a narrower bandwidth light source so as to focus the information in transform domain. Narrow bandwidth light source produces a better quality of the output image compared to the traditional LED array light source.

Keywords: Medical imaging, Fourier Ptychography, Re-focus, Wavelength, Bandwidth, light source, Portable microscope, computational imaging, point of care;

ABSTRAKT

MIKROSKOPIA E PTIKOGRAFISË FURIER - MBARTSHMËRIA DHE NJEHSIMI TË DËSHMUAR NGA PIKA E VROJTIMIT

IMERAJ, Gent

Master Shkencor, Departmenti I Inxhinierisë Kompjuterike

Supervisor: Asoc. Prof. Dr. Arban UKA

Imazheria mjekësore është një fushë në rritje që ka lindur nga nevoja për të kryer diagnostifikimin, monitorimin dhe analizën jo invazive të sistemeve biologjike. Ne jemi përqëndruar në marrjen e imazhit dhe analizën e imazhit duke përdorur mikroskopë portabël për analizën e pikës së vrojtimit dhe analizën e imazhit në njësitë e kompjuterimit portabël. Kjo tezë fokusohet në ptikografinë e Furierit, duke marrë nga përvoja e Digital InLine Holography dhe BrightField Mikroskopi, e perkur më parë në teza të tjera të autorit. FP është një teknikë e njesimit të imazhit që përdor një ndriçim matricë për të marrë një seri imazhesh me rezolucion të ulët, që përdoren për të rindërtuar një imazh kompleks, duke rezultuar në një SBP të lartë. Ka 3 hipoteza në këtë tezë që janë verifikuar / azhurnuar në lidhje me përmirësimin e FP nga metodologjia eksperimentale dhe qasja teorike. Është vërtetuar se duke fokusuar manualisht imazhet për një set të të dhënave 5x5 që do të përdoren në FP, rezultati kompleks i rezultateve ka një rezolucion të rritur. Gjithashtu, duke ndryshuar gjatësinë e valës së burimit të dritës LED kur kryen marrjen e të dhënave, ajo prodhon një imazh tjetër dalës. Meqenëse gjatësia e valës më e vogël është frekuencë më e lartë, dhe frekuenca e lartë është rezolucioni në hapësirë furier, imazhi i daljes duhet të jetë me cilësi më të mirë për gjatësi vale të vogla (jeshile ose blu). Komponenti i tretë ka vëzhguar gjerësinë e bandës së vetë burimit të dritës, duke zëvendësuar dritën LED me një burim drite më të ngushtë në spektër në mënyrë që të përqendrohet informacioni në hapësirën furier. Burimi i dritës së gjerësisë së spektrit të ngushtë prodhon një cilësi më të mirë të imazhit të daljes krahasuar me burimin tradicional të dritës LED.

Fjalë kyçe: Imazheria mjekësore, Ptikografia Furier, Fokusim, Gjatësi vale, Gjerësia e spektrit, burimi i dritës, mikroskopi portabël, imazhi kompjuterik, pika e vrojtimit;

Dedicated to the ones who raise me up

ACKNOWLEDGEMENTS

It is of my deepest honor to exhibit gratitude to my supervisor Assist. Prof. Dr. Arban UKA for the faith, responsibility and time invested on my capacity building during the 3 years of my bachelor studies and 2 years of my master studies. The model he created as a professor and as a supervisor contains virtues which I learnt from and adjusted in my character.

My thesis is a contribution to PANBiORA project that received funding from the European Union's Horizon 2020 research and innovation program under grant agreement No 760921. The project started on January of 2018 and the duration is 48 months. EPOKA University is part of the consortium led by Spartha Medical company (Strasbourg, France). The specific aim for our team is to improve existing spatial resolution by supplying a portable microscope with hardware that allows for programmable lighting. The department that is responsible for the completion of the respective tasks is Computer Engineering Department. The consortium is composed of 17 different institutions from 11 European countries. The final product is projected to serve to universities, biomaterial companies and research institutions.

TABLE OF CONTENTS

LIST OF TABLES

LIST OF FIGURES

LIST OF ABBREVIATIONS

DIHM	Digital In- Line Holographic Microscopy
PANBiORA	Personalised and/or Generalised Integrated Biomaterial Risk Assessment
LED	Light Emitted Diode
IAAL	Image Acquisition and Analysis Laboratory
EPOKA	EPOKA University
COST	European Cooperation in Science and Technology
BIONECA	Biomaterials and Advanced Physical Techniques for Regenerative Cardiology and Neurology
PoC	Proof of Concept
IP	Intellectual property
AI	Artificial Intelligence
MOHCI	Portable Microscopy employing Optimal Hardware and Computational Imaging

CHAPTER 1

INTRODUCTION

1.1. Background

1.1.1. Medical Imaging

Present field of study is related to Medical imaging, as a growing field that has stemmed from the need to conduct non-invasive diagnosis, monitoring and analysis of biological systems. With the developments and advances in the medical field and the new techniques that are used in the intervention of diseases very soon the prevalence of implanted biomedical devices will be even more significant.

The implanted biomaterials in a biological system are used as supportive units in different organs (knee, heart valve, bone support shims), which require lengthy risk assessment evaluation processes. Herein, we are working on the currently used image analysis-based techniques for assessment of biomaterial/cell interaction, their advantages and also shortcomings in order to provide biomaterials scientists and biologist working with biomaterials with a clearer view of the imaging techniques.

Emerging techniques such as utilization of machine learning and cell specific pattern recognition algorithms and potential future directions are tackled. Automation and optimization of biomaterial assessment can facilitate the discovery of novel biomaterials together with making the validation of biomedical innovations cheaper and faster. I focused on image acquisition and image analysis using portable microscopes for point-of-care analysis and image analysis on portable computing units.

Main features for medical applications:

- Bio functionality • Playing a particular physical and mechanical function (Physical Requirements: • Hard Materials • Flexible Materials).
- Bio compatibility • Concept that relates to a set of characteristics that a material must have to be used securely in a biological organism (lack of the capacity or tendency to generate cancer, lack of acceptance of an external factor that may cause rejection, lack of capacity to cause birth defects, lack of toxicity). (Jozef A. Helsen, 2010)

Researchers at Epoka University Albania are participating in a H2020 project (https://www.panbiora.eu/) to develop new microscope technology. The **"Personalised And/or Generalised Integrated Biomaterial Risk Assessment" (PANBioRA)** project is conducted under the Horizon 2020 topic titled "Development of a reliable methodology for better risk management of engineered biomaterials in Advanced Therapy Medicinal Products and/or Medical Devices".[1] PANBioRA aims at providing a comprehensive solution for the time- and cost-effective risk assessment of new biomaterials under health or disease states or a given biomaterial for each patient in a personalized manner.

1.1.2. Fourier Ptychography Microscopy

Space-Bandwidth-Product is a concept that is used by optical engineers to define the number of total resolvable pixels in an imaging system. In microscopy, SBPs of the majority of optical lenses are in the order of 10 megapixel (MP) and it does not depend on other physical parameters that will be mentioned in the later sections. Designing a microscope that would perform with gigapixel SBP is limited by the geometrical aberrations arising from increasing the size of the lens to increase the SBP. In addition, this change in the lens size is a very expensive and impractical solution to the problem. It is now when the computational power comes into play.

Fourier ptychography (FP) is a computational imaging technique that is able to bypass the barrier of SBP without involving procedures like mechanical scanning or phase measurement. The two innovations employed in this method are phase retrieving and numerical aperture synthesis, which are integrated using a unique algorithm for data combination in order to recover a high-SBP sample image that contains a complete picture of the entire light field (both intensity and phase information). The Fourier Psychograph Microscopy has become very attractive for commercial microscopy since it incorporates inexpensive hardware modification by simply using a programmable LED array instead of conventional illumination sources. Assuming that the sample is on focus, low resolution image data is collected by illuminating the specimen using the LED matrix in different angles. These images are then processed under the FP algorithm using the computational power to retrieve the final high-resolution image [2]. This permits the use of image reconstruction algorithms to further improve the resolution. The platform under development will integrate not only the image acquisition (the microscope

taking an image) but also the software that analyzes the images. The major tasks include: i) preparation of highly sensitive integrated circuits for the measurement of the response of biomaterials, ii) automated analysis of experimental data that will be extracted from images and videos employing the necessary software and hardware, and iii) integration of the developed technology into portable and user-friendly devices.

1.1.3. State of Art

In partnership with other sibling European projects, I have had the chance to conduct FTIR Spectroscopy on the biomaterials created on EPOKA laboratory premises. FTIR was conducted at the Institute of Nuclear Physics. As a huge benefit, prof. Arban UKA has been careful in continuously supporting traineeships in European scale with homologue partners for the academic staff involved but also for the students. This year I am delighted to be part of BIONECA school, part of COST programme.

All the above-mentioned opportunities have come with the passing of time, by my increased interest in Medical Imaging field, highly oriented to my better comprehension of its components. The continuous activation grew my will to conduct this thesis.

1.1.4. IP Strategy

The product of this thesis has the capability in being projected into a Prototype. To design a prototype, there are some regulations regarding the Intellectual property strategy that apply. A planning process on how to file a patent application is dictated by the requirements of the Albanian Law on Industrial Property and in particular *5.c A technical process patented under Biotechnological inventions.*

There are several patenting categories which may be considered in an IP strategy. In A prototype, one can validate: the originality of the technique; logo and brand; slogan/moto; novelty in hardware structure; designing principle etc. These categories enable the possibility to claim the authorship on a Proof of Concept with court rights. These are important essentials when working in Research and Innovation projects.

1.1.5. Patenting and Disclosure

A project is considered well advanced when it gets accompanied by a patent strategy and has good processes in place for auditing and recording results as well as checking for possible competing IP in the field that would reduce novelty or limit freedom to operate. What is crucial

with patenting is to manage the conceal of information up to the amount that it allows publishing it as a patent. It indicates that a determined competitor could probably reverse engineer the product by taking one apart and this may arise as a risk. In this situation patent protection is the only real option to try and prevent replication. Legally, the patent should contain an 'enabling disclosure' meaning that other people with a similar background in engineering (legally: a 'person skilled in the art') would be able to make the system purely by reading the patent and studying the drawings (legally: without 'undue experimentation'). Choosing a low-mass market and audience groups who will try to work from the patent, not being huge multi-nationals with strong financial and human resources is a business skill. Such a team is urged to try and keep as much information as a trade secret as is commensurate with 'enabling' the patent. The alternative strategy would be to rely on using 'trade secrets' rather than to patent. A decision on this point would be based on balancing the benefits and drawbacks of patenting and the need to keep confidential materials that might otherwise be published in academic papers.

1.2. Purpose of thesis

1.2.1 Problem statement

There is an ongoing medical need to be able to deduce the toxicity of biomaterials from the health state of cells that are placed in contact with the biomaterials. The results can be used, for example, to test the possible rejection of a medical stent before it is introduced to a patient. This analysis requires the utilization of noninvasive technique such as medical imaging. Recent development in medical imaging that acquires high resolution involves the use of: i) microscopes and ii) programmable light source on well prepared glass slides.

Existing approaches to acquire high resolution images of biological materials use LED arrays with a certain bandwidth. At the same time, these have been implemented only on glass slides where the biological samples are well prepared and frozen on the sample holder. This approach is not able to produce high resolution images for in vivo biological sample (cells). Published literature also indicate use of a bench-top microscopes that are large and sturdy. In-vitro data acquisition requires the use of microfluidic cells to hold the samples rather than freezing them. These microfluidic cells do not always fit into the working space of a commercial microscope.

1.2.2 Thesis objective

This thesis aims to create a comprehensive guidebook for students on the operation of Fourier Ptychography by critically judging on this technique's portability and computation features. Both these two branches are observed and interpreted through point-of-care analysis to better visualize the advantages and limitations of such approach to modern microscopy.

The specific objectives of the thesis are:

- ◊ To comment on the structure of a portable microscope for point of care analysis
- ◊ To build a commentary on FP mathematical apparatus and computational algorithm
- ◊ To illustrate the full image acquisition cycle of FP and its coded programing
- ◊ To expand on the breakthroughs and limitations faced by such technique
- ◊ To conclude a working principle for non-invasive microscopy technique with clear workflow

1.2.3 Thesis design

This thesis is divided in 7 chapters. The organization is done as follows:

In Chapter 1, the problem statement, thesis objective and scope of works is presented. Chapter 2, includes the literature review, extracted problems and future work proposed. Chapter 3, consists of the theoretical approach towards understanding the mathematical apparatus. In Chapter 4, the experimental results and methodology are conducted and tested. Chapter 5 describes experiments with nanofibers, imitating a biomaterial. Chapter 6 has a novelty research thought on a future work. In chapter 7, conclusions and recommendations for further research are stated. References and appendices are added in the end.

1.2.4 Scope of works

Throughout my 3 years of engagement with PANBiORA project / IAAL, I have kept note on some of the most wide-spread techniques of portable microscopy.[3] An overview on the microscope techniques tackled by me are *(Note: Only FP is part of this thesis, where the other 2 techniques have been subject of student's bachelor thesis, with reference to my partial reports and supervising, led by prof. Arban UKA):*

Digital In-Line Holographic microscopy	DIHM is a lens-free microscopy system, which means that the image is projected directly onto CMOS when illuminated by the light. Such technique projects everything in the scope of light travelling area, constrained by the field of view of the CMOS. When the sample is projected onto the CMOS, due to a certain height, distance sample CMOS, what the camera registers is the holographic (magnified) image of the sample. This holographic image gets affected by light circular ever-expanding propagation by creating ripples. DIHM aims to register the process and reverse the ripples to purely pass the phase information into amplitude. The technique has resulted effective in cases of clean pathway between light source and CMOS. The results of such technique are registered in my bachelor thesis and in the thesis Bachelor thesis of Stela Lila (2021)[4], Sara Rustemi (2020)[5].
Bright-field microscopy	The standard method is **bright field** microscopy. It is appropriate for observing a specimen's natural colors or stained sample observation. The system uses a regular light-gathering objective / lens, which standardizes the wave direction and magnifies the sample. Bright-field microscopy makes use of the focal point of the lens, to focus a single cross-cut of a sample, found in the focal length of the objective/lens. Bright-field is highly selective in Z-stage, which means that depth of focus is narrow and the image can easily loose in Z-scanning. To avoid such limitation, extension tubes have been utilized. They absorb the light and do not reflect it backwards, by preserving the intensity and they are great magnifiers. In addition, due to their lengthy shape, they are able to extend the depth of field, by giving more freedom of movement with the Z-stage without getting out of focus. The results of such technique are registered in periodic reports I have compiled for PANBiORA project and master thesis of Latif Xeka (2019)[6].
Fourier Ptychography microscopy	Fourier Ptychography is explained in detail along the whole thesis. It is a complete overview of the work of many students, me and prof. Arban UKA. I have assisted his supervision in the following bachelor thesis: Albert Kopaci (2020)[6], Ismiana Qose (2021)[7], Besmir Shehu (2021)[8], Bjorna Qesaraku (2021)[9].

1.3 Point-of-care analysis

From the scientific point of view, microscope in itself is a combination of many natural observations which have been explained by human in centuries through equations binding it to the laws of Optics. Microscope is an instrument used to monitor objects in a small size which are difficult to be detected by human eye and to gather qualitative and quantitative information. Having knowledge on the optics field, it opens way to utilizing the microscope in an efficient manner. But before using a microscope for a specific application, it is needed to take on consideration some important parameters which play a key role on the performance and requirements.

In the same way, to create a microscope, there are some feature of its building parts that need to be optimized so as to have the highest gain from the device. A microscope has to cover a wide area (Field of View), it needs to produce the necessary magnification (Magnification coefficient), depth of focus (sensitivity) and also the light propagation should appear to us almost uniformly for better approximations (Numerical Aperture).

Field of view

The field diameter of an optical light microscope is the field number measured at the intermediate image plane, which is the field view diameter in mm. Usually the field number is mentioned on the eye piece of the microscope. The greater the magnification, the narrower the field of perspective of the microscope [1] The microscope field of view is found with the following formula:

$$F\text{ield of View} = \frac{\text{Nb of pixels} * \text{Pixel size}}{\text{Objective Magnification}}$$

Nb. of Pixels refers to the CMOS size, the same as pixel size does. If an additional lens is used on a stereo microscope, this lens ' magnification factor should also be used[1]:

$$F\text{ield of View} = \frac{\text{Nb of pixels} * \text{Pixel size}}{\text{Objective Magnification} * \text{Auxiliary Lens Magnification}}$$

Magnification coefficient

Magnification on a microscope relates to an observed object's quantity or degree of visual enlargement. Magnification is evaluated by multiples, such as 2x, 4x and 10x, which indicate that the object is enlarged twice as large, four times as large or ten times as large, respectively[1].

The peak magnification goes up to 1,500x for a conventional light-based microscope; beyond that, objects under perspective become excessively fuzzy because light's wavelengths restrict image clarity. On the other side, electrons have significantly shorter wavelengths. According to Auburn University, electron microscopes produce useful images with magnifications up to about 200,000x [1].

Depth of focus

The focal depth refers to the depth of the specimen layer that is simultaneously in sharp focus, even if the distance between the objective lens and the specimen plane is changed by microscopic observation and shooting of the specimen plane. As human eyes differ separately in the capacity to adjust their focus, the perception of the focal depth of each individual differs. The Berek formula is currently usually used as it provides a focal depth value that often coincides with that acquired through experiments [10]

$$\mathrm{DoF} = \frac{\omega * 250000}{\mathrm{NA} * \mathrm{M}} * \frac{\lambda}{2(\mathrm{NA})^2}$$

where

- ω is the resolving power of the eyes
- M is the total magnification
- λ is the wavelength

Numerical Aperture

The light that passes through the mask (the plane of the object) diffracts from different angles. Because of a lens of a certain size positioned at a certain distance from the mask, there is a certain maximum α diffraction angle for which the diffracted light simply makes it into the lens. The lens misses the light that emerges from the mask at bigger corners and is not used to form the picture. The most useful way to define the lens aperture is by its numerical aperture, described as the sine of the maximum half-angle of diffracted light that the refraction index of the surrounding medium can enter into the lens moments[11]

$$NA = n \sin \alpha$$

There is an object side and an image side numerical aperture for a lens with magnification, and the proportion between the two is the magnification factor[11].

CHAPTER 2

LITERATURE REVIEW

2.1. Introduction

The Literature review consists of a database of information collected throughout three years of working on the project. Being a field of immediate research [12][13]and in urge need of upgrading[14], the literature review has been yearly taken into consideration in order to provide the most modern technology adaptions on the Portable Microscopy for Fourier Ptychography, being in line with the equipment's found / ordered at the laboratory premises of EPOKA University. Researchers have focused on portable imaging systems over the last two decades. Among distinguished research groups are:

- Ozcan group (UCLA) https://innovate.ee.ucla.edu/
- Laura Waller group http://www.laurawaller.com/research/
- Tian Lab (Boston University) http://sites.bu.edu/tianlab/research/
- Cedric Allier group (France) https://fr.linkedin.com/in/c%C3%A9dric-allier-3a77796
- Johan Danzl group (Austria) https://ist.ac.at/en/research/danzl-group/

The thesis has taken into consideration a literature of more than 50 papers / publications / books that altogether construct the big piece of the methodology in focus: FPM. Chronologically ascending, Literature review section is organized in identifying the most prevalent problems which have been able to be solved and the ones that haven't been solved, but a future work has been proposed as an alternative. After acquiring the present state of the global research teams, the research group at EPOKA has identified a research gap, which through some research questions is tried to be addressed.

2.2. Summary of literature reviewed

Zheng Guoan [15][16] and his team have been the first to report the imaging method which they termed "Fourier ptychographic microscopy (FPM)", in 2013. In their paper, they discuss that through a mathematical apparatus they were able to produce a high-resolution image from iteratively stitching together in Fourier space a series of low-resolution images variably illuminated. They make use of a wave front correction strategy to correct for aberrations and digitally extend the microscope's depth of focus beyond the physical limitations of its optics. Their microscope structure had features: spatial resolution $= 0.78\,\mu m$; field of

view $\sim 120 mm^2$; depth of focus $= 0.3\, mm$ (characterized at $632\, nm$). The imaging technique described here converts the fundamental issue of high-throughput, high-resolution microscopy from one that is bound by the physical constraints of the system's optics to one that can be solved by computing.

Tian Lab [17] is the working group that has shared the MATLAB code and the datasets that may be simulated. The provided MATLAB code is useful, which is a synthesis of the equations utilized in the approach. In Tian's work, the hardware setup introduces a matrix illumination with a programmable LED array, which is useful to have a fixed-distanced LEDs which iteratively turn ON, by allowing to precisely measure the mathematical parameters such as: optical path distance, angle of illumination etc. They make use of multiplexed illumination (many LEDs in a single time) to achieve similar results by reducing the data acquisition time.

These 2 pioneers initiated an out-of-the-box way of thinking, were other researchers started to grasp into. In 2014, some researchers advanced to the Fourier space in Medical Imaging by trialing remarkable application on image reconstruction of unresolved images. [18][19] [20] Some of these properties are described in my Bachelor thesis on Digital-In Line Holographic Microscopy.[21] The book of Osgood, B. [22] on Fourier and its application contain a highly recommended study guide regarding what Fourier domain consists of and how it works, with concrete examples and exercises. Vasista, Adarsh B. discusses in his paper too regarding Fourier Optical plane by connecting Intensity,[23] wave vector,[24] phase,[23] and polarization[25] as the most important parameters of light beam in providing unique information about the light-matter interaction [11][26].

In the last 3 years, there have been many publications regarding the Fourier Ptychography Microscopy technique, which have tried to optimize the hardware[27] [28] [29] [30] [31]–[34]and software content.[35] [36] [37] [38][39]–[42] Sun, J. and his team have discussed the FPM method to come in need of the high-throughput quantitative phase imaging (QPI), which is essential to cellular phenotypes characterization. Other researchers that have worked with cell-based environments [43][44]. Despite the breakthrough, they raise the concern that the way how the light is illuminated in traditional FPM might not be the most efficient way because it requires a large dataset, thus consuming a large amount of time. The optical-transfer-function (OTF) research revealed in their high-speed FPM[45] study that the low-frequency phase information can only be successfully retrieved if the LEDs are exactly positioned at the

frequency space's edge of the objective numerical aperture (NA)[46]. By knowing this, they obtain only 4 low-resolution images corresponding to 4 tilted illuminations matching a $10\times$, $0.4\ NA$ objective, When reconstructed, they claim to be able to monitor in vitro (cells are alive [47]) Hela cells mitosis and apoptosis at a frame rate of $25\ Hz$ with a full-pitch resolution of $655\ nm$ at a wavelength of $525\ nm$ (effective $NA = 0.8$) across a wide field-of-view $= 1.77\ mm^2$, corresponding to a space-bandwidth-time product of $411\ megapixels\ per\ second$. [48].

When the light is illuminated in center and the image gets placed into objective's focus (from the lens equation), it may be defined the optimal path of light travelling for the image to be in the focal distance.[49][50] Now, when a light source different from the one in the center is lit on, the optical path changes, thus shifting the image from the focal point and disturbing the focus. This limitation from physics has been discussed in papers, where they describe the edge aberrations as" Vignetting effect" and they try to extend the depth-of-focus, so as to allow a displacement of image without getting out of the focal point. [51], [52]

2.3. Literature review: extracting problems & future work

After the timeline growth of Medical Imaging with focus on Fourier Ptychography, it can be stressed that the technique in itself tries to bloom beyond the physical limitations of the nature that the humans have put along the centuries in mathematical bounds. Some of them were able to deduct ways how to do it, and some others tried to optimize or open a new field of study. From the above mentioned key literature and further, a grouping of the following categories is described:

The resolved problems that were tackled from the research fields:

- Led array substituting illumination matrix for more accurate performance
- Reconstruction of unresolved images in Fourier plane by computing power
- Extended depth of focus with the FPM technique
- Decrease of acquisition time by acquiring certain images at essential positions
- High-speed high-throughput imaging of in vitro live cells

The unresolved problems / future work that were addressed as possible fields to extend the research area are:

- Passing from the testing on commercial microscopes to portable microscopes
- Large dataset requirement in conventional FPM significantly limits imaging speed, which needs to be reduced
- Optimum illumination scheme for high-accuracy phase imaging in FPM remains unclear, how the matrix of light should be arranged
- Vignetting effect – edge aberration due to optical path change of the light source

2.4. Research gap

From the literature review, it is concluded that the many limitations occurring from the mathematics in Imaging, computational power has become a very powerful asset in surpassing these obstacles. Through coded algorithms, it is able to quantitatively and qualitatively show a measurable output which would have not been able to be obtained from direct microscopy techniques. Thus, Computational Microscopy is a key feature of modern Medical Imaging. To be optimized, there remain 3 main branches which are: Portability, Illumination, In-vivo.

Many of the papers, they utilize conventional microscopes, heavy and large in size. The thesis is built upon experiments and results on portable microscope only, by discussing its optimizations and advantages.

In regard to the light illumination, the LED matrix has been the most popular equipment among the research groups in FPM. But LED in itself is inefficient from the aspect of spatial resolution (discussed further in chapter 3). Other light sources with increased spatial resolution need to be tested to compare the results.

As mentioned in the summary of Literature review, developing non-invasive techniques on in-vivo biological samples is a key feature of modern microscopy. This detail has been taken in consideration for the thesis, by analyzing some nanofibers self-produced at EPOKA laboratory, to monitor their chemical compounds formed and if there are traces of undesired material (zeolites).

2.5. Research questions & hypotheses

The research gap of this thesis directly gives a hint on what aspects of today's FPM research are found within the optics' of R&D laboratories around the world. From the categorization above, it concludes that this thesis needs to discuss upon 3 different research questions and rise 3 preliminary hypotheses to be answered upon the completion of the methodological aspect & conclusions.

Below are written the 3 hypotheses together with the 3 research questions that this thesis demands to give an interpretation in compliance with measurable results.

Research question #1:

◊ Does portable microscopy meet all the necessary requirements to conduct a modern medical Imaging Acquisition by integrating computational algorithms and need for re-focusing of the dataset?

Hypothesis #1:

◊ Portable microscopes are composed of vital parts which reduces the hardware components and still extract the necessary information from the sample being studied to be able to quantify it in high resolution through coded algorithms. By increasing the computational complexity, it can be artificially increased the physical limitations arising in microscopy. Re-focusing of the optical path increases the output resolution in an improved factor.

Research question #2:

◊ Is Fourier Ptychography Microscopy dependent on illumination frequency and bandwidth dependent on the wavelength of the light source, with respect to the visible spectrum?

Hypothesis #2:

◊ FPM works better if the LED is replaced by a light source with narrower bandwidth, which would naturally increase the resolution of the image datasets, which when reconstructed would produce a higher precision in the output image. Different wavelength of the spectrum produces different resolution, where a comparison between red, green and blue is made.

Research question #3:

◊ Does portable microscopy using FPM has the need to be focused before processing algorithm of the low-resolution images?

Hypothesis #3:

◊ FPM implemented in a portable microscope is dependent on the optical path length, which acquires to manually or automatically adjust the focus distance on every iteration in order to provide a higher quality image of the sample.

The 3 hypotheses have been addressed with experimental results and hypothesis-oriented methodology. It means that the hypotheses are initially discussed in Chapter 1 and Chapter 3 from the theoretical point of view, to be probed in Chapter 4 and Chapter 5 with a validated workflow and work plan.

CHAPTER 3

THEORETICAL APPROACH

3.1 Wave propagation & Diffraction theory

Fourier optics discusses light propagation using Fourier transform methods in optical systems. Since many operations in the studied area are linear and spatially shifting invariant, these methods are very helpful. They form the foundation for the analysis and design of computational and optical imaging systems.

3.1.1 Propagation of light: Maxwell's equations

Although the classical wave description of light is as a transverse electromagnetic wave, many effects can be studied using a scalar rather than the full vector wave equation. In free space, we have

$$\boldsymbol{\nabla} \cdot \boldsymbol{\nabla}\psi = \frac{\partial^2\psi}{\partial x^2} + \frac{\partial^2\psi}{\partial y^2} + \frac{\partial^2\psi}{\partial z^2} = \frac{1}{c^2}\frac{\partial^2\psi}{\partial t^2}$$

In this equation ψ represents a component of the electric or magnetic field. For monochromatic, coherent light, we can write

$$\psi(\mathrm{x},\mathrm{y},\mathrm{z},\mathrm{t}) = \psi(\mathrm{x},\mathrm{y},\mathrm{z},0) * e^{-i\omega t}$$

Substituting this into the wave equation, we obtain Helmholtz's equation:

$$\frac{\partial^2\psi}{\partial x^2} + \frac{\partial^2\psi}{\partial y^2} + \frac{\partial^2\psi}{\partial z^2} = -k^2\psi$$

where $\omega/k = c$

If it is considered that the propagation is nearly parallel to the z axis, so that

$$\psi(\mathrm{x},\mathrm{y},\mathrm{z},\mathrm{t}) = f_z(\mathrm{x},\mathrm{y},) * e^{\mathrm{j}kz}$$

solving the paraxial equation would yield to:

$$F_z(u,v) = F_0(u,v)exp\left[-\frac{j2\pi^2}{k}\,(u^2+v^2)\,z\right]$$

The exponential term is called "Propagator term" and it defines how the light pattern changes as distance z varies. This equation is an integral part when the Transform domain is

analyzed. Similar to the bachelor thesis on DIHM technology, the MATLAB code tries to calculate the z in order to define what region is being focused from the lens system so as to update that patched area in transform domain to the final output.

3.1.2 Fourier optics - Visualization

Through the years at the studies, Fourier transform has been a fundamental mathematical apparatus in analyzing every analog function, being projected in frequency domain. In this section, an explanation on what is the Fourier domain and what are the main formulas of it, is described. Imagine a sound wave, which is a pure cosine wave, traveling at frequency f1 = 3Hz. Add to it another sound wave, cosine-shaped with frequency $f2 = 5Hz$. Now, merge those two signals to produce a single sound wave with function $cos\_wave\,(t) = cos\_wave1(t) + cos\_wave2(t)$. Plotting it in Python (see: APPENDIX B) would give a wavy function, which can be very hard to be decomposed into the previous sum with naked eye.

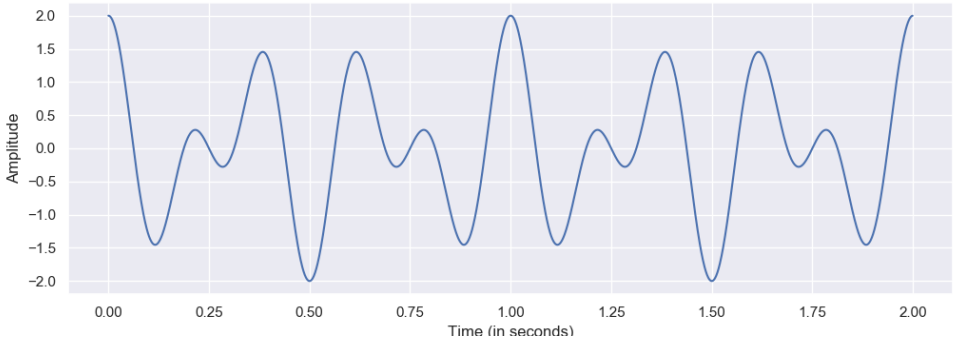

Figure 1 The sound wave when adding two cosine waves at different frequencies

They key idea of extracting the information, would be to take this graph and wrap it up around a circle. Imagine a rotating vector, which Is centered at the origin and it draws the amplitude of the function as it updates with the time. In the graph below there are shown a variety of rotations with different frequencies for the above function (see: APPENDIX B[53]).

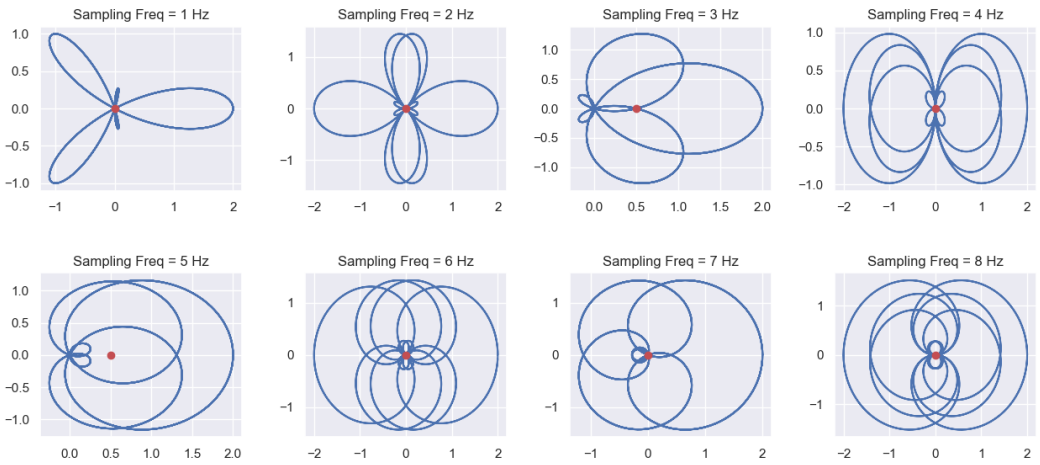

Figure 2 The sound wave wrapped around a circle in frequencies from 1 Hz to 9 Hz

The graphs above have in their plotting a red dot which is formed by keeping track of the mean value of the vector's amplitude and phase. Think about the dot as the weight of the function. In the figure below, there is found a plotting of the weights value for a frequency range from 1 Hz to 9 Hz with step size 0.01. *(see: APPENDIX B for full python code).*

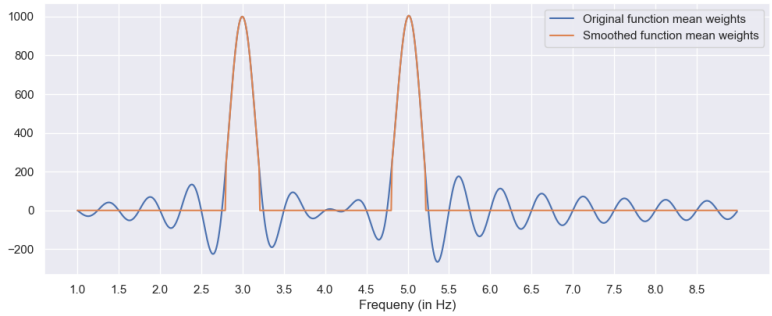

Figure 3 Mean weights for the function sampled in frequency range 1 – 9

It is observed that at the frequency $f1 = 3Hz$ and $f2 = 5Hz$, the graph reaches the maximum weight. Here, it is deducted that the sound wave in Figure 1 is a composition of two different waves which are added up, in their unique frequencies $@3Hz\ and\ @5Hz$.

This is basis how to understand the Fourier Transform. What it happnened is that the linear graph was represented in a 2D circle by wrapping it around. In order to represent each point of the circle, a sum of sine and cosine is used for unit circle. Recall the Euler's equation, which describes such an expression in the exponential form:

$$e^{i*2*\pi*f*t} = \cos 2*\pi*f*t + i*\sin 2*\pi*f*t$$

Since the rotational vector in Figure above measures the amplitude of the function (in the clockwise direction), it would be obtained an expression such as $cos\_wave(t) * e^{-i*2*\pi*f*t}$. This would produce the exact amplitude in the circular shape. The last detail to produce the Mean Weight Function in Figure 2 is to sum up all the samples of the signal in time domain. Smaller the step size (Δt), better the resolution in frequency (explained in 3.1.3 The Uncertinity Principle). The limit of Δt while it goes to zero is dt. And the final function that represents the frequency domain of the time-dependent signal, would have the form of:

$$F(\omega) = \int_{t1}^{t2} \cos\_wave(t) * \ e^{-i*2*\pi*f*t} * dt$$

And this if the Fourier transform formula, the way it is derived. Note that to find the mean weight, it is needed to average the value, thus a division by $1/\ 2 * \pi$. This is how the Fourier formula is able to decompose a summed signal in time, in a graph of specific frequencies.

3.1.3 The Uncertainty principle

The theoretical physicts, Werner Heisenberg, articulated in 1927 his hypthesis on the uncertainty principle stating that the more accurately we measure the velocity of a particle, the less accurately we can measure its position in space and vice-versa. There is an important flow of understanding to follow for accurate applying of this theorem.

All the objects in the world have 2 natures, behaving as a wave & behaving as a particle. Particles by definition exist in a single place, at any instant in time. Waves, on the other hand, are disturbances spread out in space, of which we can identify features. Wavelength is essential for quantum physics, because from there it can be measured the momentum of an object. The $moment\ = mass * velocity$, which indicates that the greater the mass, higher the frequency, smaller the wavelength. This is why we do not notice the everyday nature of the object. In the macro world, if we throw a ball upwards, the wavelength would be very small to measure it (it is almost impossible to measure it with our scaling devices). On the other hand, in the quantum world, the atom has a lower mass and we can calculate its frequency and define wavelength. If we have a pure wave, we can measure its wavelength and momentum.

Figure 4 The nature of Objects (particle and wave)

Heisenberg's Uncertainity principle is expressed in a single equation:

$$\Delta x * \Delta p \geq \frac{h}{4 * \pi} = \frac{\hbar}{2}$$

where h is the Planck's constant, $\boldsymbol{h} = 6.62607015 * 10^{-34}\, J * Hz^{-1}$.

Expressed in words: *"The more accurate you know the position (the smaller the uncertainity in position Δx is), the less accurately you know the momentum (the higher the uncertainity in momentum Δp is); and vice versa".*

To conclude the example and this theme, it can be extracted that a low-resolution acquisition in time domain, results in a high resolution in frequency domain, this in regard to a large mass. As it is extracted in Chapter 4, larger the image acquired in a low resolution, the higher its accuracy (information) in Transform domain. This explains a bit the genesis of the Fourier Ptychography Microscopy, basis and a simple PoC.

3.1.4 Index of refraction

The way how microscopy works is that it defines an optic system so as to analyze a sample. The sample may be either artificial or biological. If it is biological, it can be stained or incubated (in vitro). On all the cases, the sample needs to be placed on a holder (glass in general) so as to be positioned in the objective view.

When doing the placement in such way, an addition thickness is added to the sample's mass which effects the focal point of the structure and its depth of focus. In simple words, the sample is a 3D material which means that it has a height. Adding the glass slide thickness, it creates a medium which would play a role in the z-stage scanning of the microscope's depth of focus by shifting it upwards or downwards.

In the case of the glass slide, due to the change of the index of refraction, it is discussed on what effect does it bring to the beam wave when propagating from the source (medium with index of refraction n1) towards the sample (medium n2) and again up to the objective / camera (medium n1).

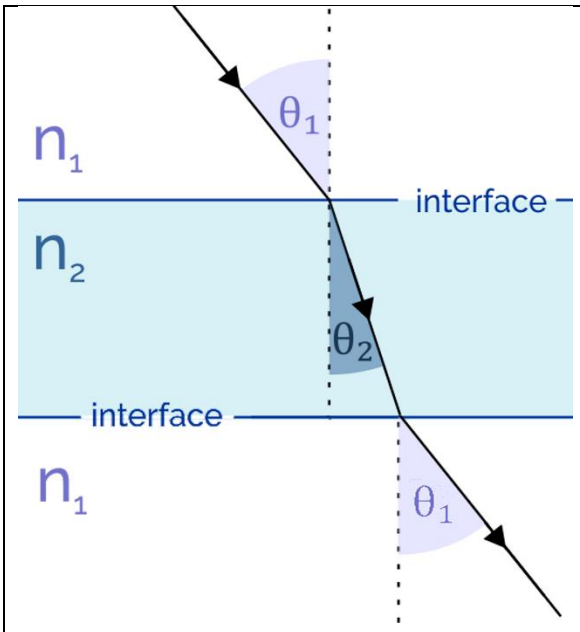

Figure 5 Light beam propagation when hiting the sample and being projected to objective

The reasoning helps understand that due to the thickness of the glass slide, it is artificially obtained a $+\Delta x$ of the beam, by delaying its expansion. Also, it is logical to say that different angles would affect a non-linear Δx distribution of the light beam after passing the 2nd interface.

Suppose the light beam with wavelength λ is coming towards the sample to lit it with an angle θ_1. The index of refraction for air is considered to be $n_1 = 1$. At the moment of the interface surface, the light beam will change its angle of inclination by passing to θ_2. This change happens due to Snell's law on refracting when there is a change in the medium's index of refraction. In the case of medical studies, the 2nd medium is in general glass slide. Glass has $n_2 = 1.52$. To find θ_2, it is made use of Snell's equation:

$$n_1 * \sin\theta_1 = n_2 * \sin\theta_2$$

Since $n_2 > n_1$ by a factor of 1.52, it means that $\frac{\sin\theta_1}{\sin\theta_2} = 1.52$. The focus of analysis is the horizontal cathete, which can be proved that it is delayed and shortened compared to if the beam would have gone directly without the medium change.

3.1.5 Vignetting effect

The coherent microscopic structure is approximated in the normal model of Fourier ptychographic microscopy (FPM) by being taken as a linear space-invariant (LSI) with transfer function defined by a complex pupil function of the target. Nonetheless, under actual experimental conditions, when the sample is illuminated by the LEDs some unexplained "semi-bright and semi-dark" images with a clear vignetting effect can be observed. Obviously, these incomplete images do not fit with the LSI model, and may seriously deteriorate the consistency of reconstruction. In this paper Chapter 4, it is investigated the cause and effect of model misfit based on ray-dependent and rigorous analyzes of wave optics, which is going to make use of the 3.1.4 Index of Refraction

The theme shows that the LSI model breaks down because of diffraction at other stops or apertures associated with different lens components for a realistic FPM microscope with a small magnification objective and a wide field-of - view (FOV). For quantitative analysis, a modified version of the linear space-variant (LSV) model is used. Countermeasures are also provided and experimentally tested to circumvent or mitigate the artefacts of reconstruction caused by vignetting.

For better reconstructions an adaptive update order and a mathematical strategy is suggested and demonstrated. The thesis offers a deeper insight into the vignetting effect on wide-FOV imagery and provides a valuable guide to easily achieve enhanced FPM reconstructions that circumvent the adverse effect.

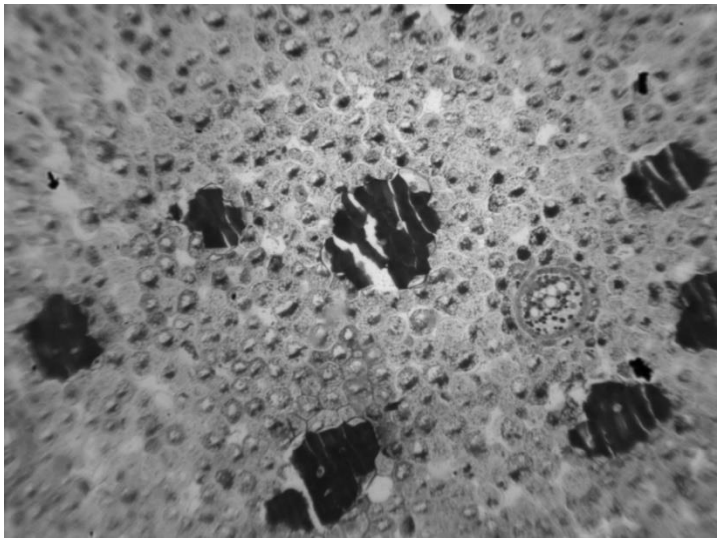

Figure 6 Image of Fern Ribozome taken at lab premises, with blurred edges

3.1.6 Effect of re-focusing

In order to produce a high-resolution image after the reconstruction process, the information in each measurement must be encoded redundantly such that the LEDs close to each other overlap in at least 60% coverage of the Fourier space of the sample [54]. This results in poor input to output ratio since approximately 10 times more pixels are acquired compared to the number of pixels that are reconstructed. The collection of raw data images may still be overwhelming for the computer, depending on the type of camera and the image quality.

To rescue the computer from drowning in data less LEDs will be turned on to cover the full image space of the sample [54][55][56]. Furthermore, improved algorithm that accounts for the errors in such angle change of illumination and spatially multiplexes the measurements only inquiring the ones that contain the most important information will still be able to produce a high-resolution image at the end. In 3D samples the light field refocusing is being understood intuitively as the way to compensate and correct for the geometrical shift that occurs during the plane wave propagation. This shift for a relatively thick sample is shown in Figure 7. The analysis of such shifting will be explained further by means of geometry using similar triangles.

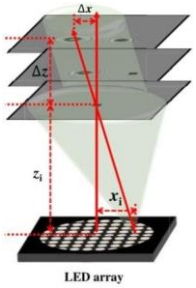

Figure 7 Geometrical shift during the plane wave propagation

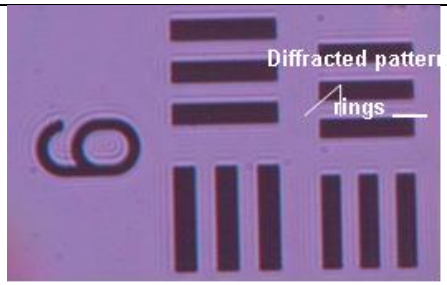

Figure 8 Diffractions and phase effect as result of illumination angle change

The illumination of LED located at xi position causes he intensity to shift from the original position in the plane of focus by a distance of $\Delta x = xi * \Delta z / zi$ where Δz is the thickness of the sample [57]. Phase effect and diffraction cause the light to deviate from the straight lines that predict the alignment using geometrical optics. This can be observed at the ring like diffraction patters that surround each dark line as shown in Figure 8. The larger the angle is, the more visible the rings are [58]. In order to minimize these shifting in focus of the sample, this thesis proposes the manual adjustment of the focus by using a step-controlled motor with high precision.

3.2 Lambda & light intensity

The visible white light consists of several colored radiations that can be separated by a prism: their corresponding wavelengths range from 400 to 700 nanometers (one nanometer is one thousandth of a micron).

The red element of a white light can be selected through a filter; the spectral richness of the red light thus acquired is less than that of the white light, because the filter only enables the wavelengths in the red to pass (e.g. 650 to 700 nm, from light red to dark red).

In physics, intensity is the power transferred per unit area, where the area's directivity is measured perpendicular to the energy propagation direction on the plane. It has units of watts per square meter (W / m2) in the SI system.

The term "intensity" as used here is not synonymous with "strength", "amplitude", "magnitude", or "level", as it sometimes is in colloquial speech.

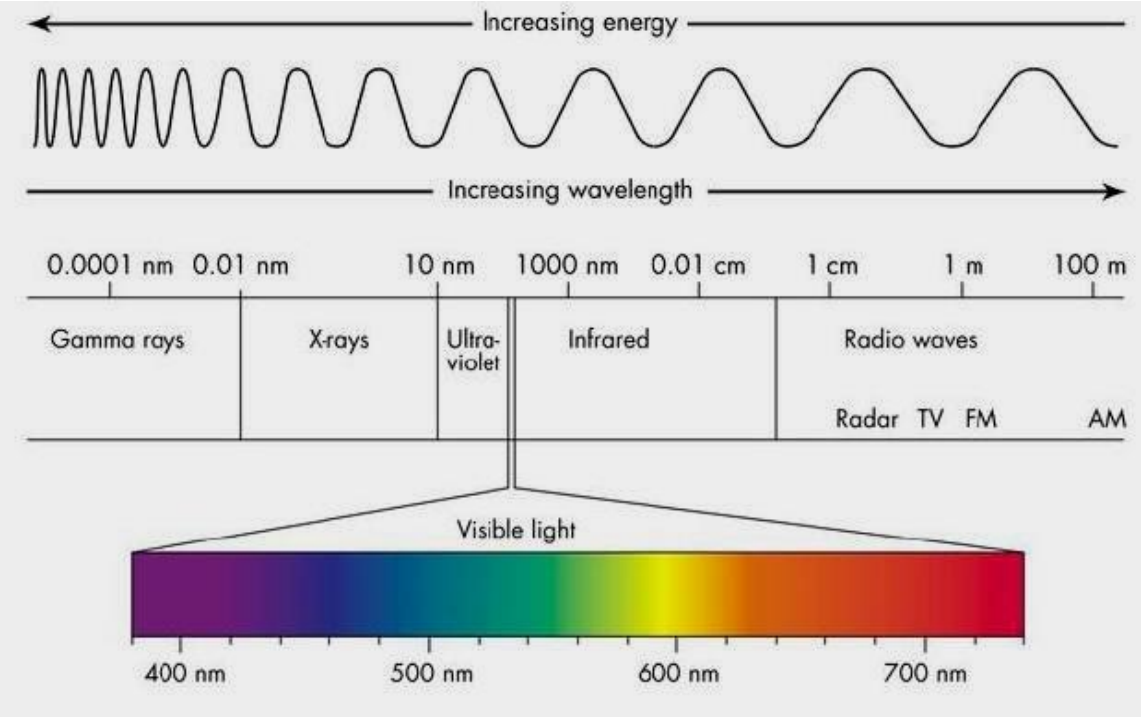

Figure 9 The Electro-Magnetic Light Spectrum, src [59]

3.2.1 Laser as a light source, properties

In the thesis, laser beam has been used as a light source at the beginning of year 2019. The laser has some features which are necessary for the microscopy, such as “in phase transmission of light”.

The coherence of the laser light is both spatial and temporal.

Spatial coherence: At a given moment, all points perpendicular to the laser beam in the same plane are in the same phase state (same electromagnetic field value and orientation).

Temporal coherence represents the fact that several light waves subsequently emitted from the same source point stay in phase: this feature and, of course, strongly associated to the (almost) monochromatic appearance of laser light.

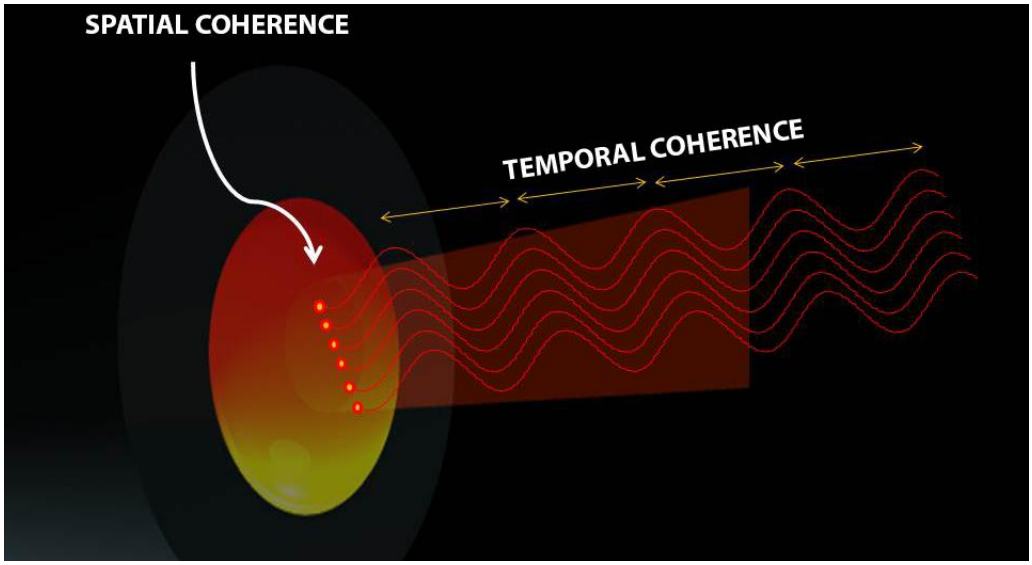

Figure 10 Coherence of laser beam

Thus, when we used laser, the bandwidth is very narrow. This helps a lot the process due to the functioning of reconstruction algorithm, which requires the information in frequency to be at maximum. The laser resources at laboratory are:

Table 1 List of laser equipment’s found in IAAL Laboratory

WAVELENGTH	PART NUMBER	POWER [WATT]	VOLTAGE INPUT [V]
405NM	38-1034-ND	20mW	5V
650NM	38-1007-ND	5mW	-
650NM	1528-1391-ND	5mW	2.8V ~ 5.2V
905NM	475-3533-ND	30W	5.3V

3.2.2 LED as a light source, properties

A light Emitting Diode (LED) is an optical semiconductor device that emits light when voltage is applied (it converts electrical energy into light energy). The LED resources at laboratory are:

Table 2 List of LED equipment's found in IAAL Laboratory

WAVELENGTH	PART NUMBER	VF MINIMUM VALUE	VF MAXIMUM VALUE
RED 640NM	GF CSHPM2.24-1T3T-1-0	1.90 V	2.05 V
GREEN 525NM	LT E6SG-AABB-35-1-Z	2.50 V	3.40 V
BLUE 470NM	LB Q39E-L2OO-35-1	2.85 V	3.00 V
CYAN 490NM	SP-05-B4	2.10 V	2.50 V
VISIBLE LIGHT	32x32 RGB MATRIX LED	3.30 V	5.40 V
VISIBLE LIGHT	16x32 RGB MATRIX LED	3.30 V	5.40 V

Output characteristics of LED

The quantity of output light emitted by the LED is directly commensurate with the quantity of forward current flowing through the LED. The higher the forward current, the higher the output light.

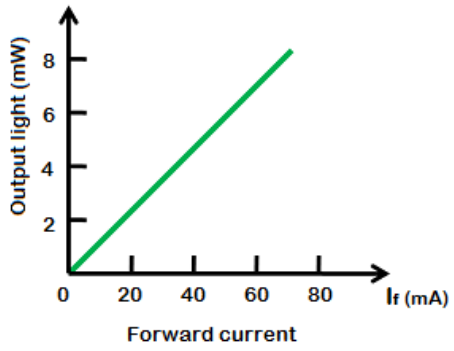

Figure 11 Forward current vs output light of LED

Advantages of LED

The intensity of light emitted by LED is dependent from the current (A) flowing through the LED. LED light can therefore be readily regulated by varying the current; light-emitting diodes consume low energy; LEDs are inexpensive and simple to execute; small size; LEDs have longer service life; they work very quickly. In a short time, they can be switched ON and OFF; LEDs can emit distinct colors of LED. The MATRIX is a programmable light array which is very helpful in FP since it can iteratively follow a pattern at well-defined distances.

3.3 Theory of proposed models & Mathematical apparatus

3.3.1 Model: Fourier Ptychography

The major parts of the computational microscope are: i) array light source, ii) sample, iii) objective/lens and iv) CMOS sensor. Having these static components in our structures, other components have been tested too, to improve qualitative and quantitative features. Since the structure is presented by an array of bright-field microscopy images, then the Mathematical Apparatus used for low-resolution images is the **lens equation**, $\frac{1}{f} = \frac{1}{d_0} + \frac{1}{d_i}$, and **magnification equation Mag** $= \frac{d_i}{d_0}$, where $\mathbf{d_o}$ is the distance lens-object, $\boldsymbol{d_i}$ is the distance lens-image and, **f** is the focal length.

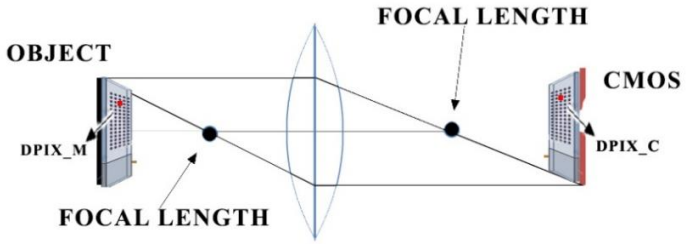

Figure 12 Mathematical System of the low-resolution images

Computational Microscopy scheme has been tested by adding some components with their respective expectations: i) 32x32 RGB LED Array (Adafruit: ID 607, 50 EUR, to obtain a large dataset of max 1024 images), ii) aperture (Edmund Optics: 53-907 & 57-574, 80 EUR, to increase contrast and depth of focus), iii) light diffuser (Edmund Optics: 35-860 & 47-988, 139 EUR, to equally spread the light above the sample for better illumination).

Cameras used for this structure of the microscope are 4:

A. Basler acA4600-10uc (ID: 106538)
   Pixel size: 1.4um, Sensor size: 6.5 mm x 4.6 mm, color, 439 EUR
B. Basler daA2500-14um (ID: 106693)
   Pixel size: 2.2um, Sensor size: 5.7 mm x 4.3 mm, mono, 149 EUR
C. Basler daA2500-14uc (ID: 106695)
   Pixel size: 2.2um, Sensor size: 5.7 mm x 4.3 mm, color, 149 EUR
D. Basler puA2500-14um (ID: 106957)
   Pixel size: 2.2um, Sensor size: 5.7 mm x 4.3 mm, mono, 159 EUR

3.3.2 Theory of the working principle

Time domain | **Transform domain**

Step 1: Obtain N low resolution images from LED matrix illumination.

Step 2: Initialize the high-resolution image, as complex number, $\sqrt{I_h}e^{i\emptyset_h}$

DFT

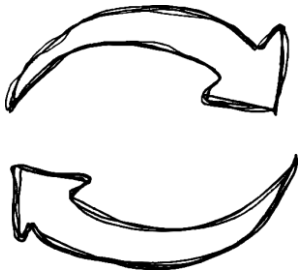

IDFT

Step 3: Generate a low-resolution image (the center of dataset) as the image which will be iterated, $\sqrt{I_l}e^{i\emptyset_l}$

Step 4: Calculate I_M from every I_l and update the corresponding region of $\sqrt{I_h}e^{i\emptyset_h}$ in Fourier Space. Repeat it for N images of dataset.

Step 5: Output is the image computed in Giga-pixels!

Since it is being worked with low-resolution images in Time domain, and they are modified in Transform domain, then the Law of Uncertainty arises as a reference point of view: Heisenberg equation

$\Delta \mathbf{x} * \Delta \boldsymbol{k} = \frac{\boldsymbol{h}}{\boldsymbol{4\pi}}$ where $\boldsymbol{h}$ is Plank's constant

Field of View $\boldsymbol{X} = \Delta \mathbf{x} * \boldsymbol{N}$ -> Real Domain – Object Plane

$\boldsymbol{K} = \Delta \mathbf{k} * \boldsymbol{N}$ -> Transform Domain – Image Plane

These upper equation, come to help by stating that:

$\boldsymbol{Larger\ Information\ in\ Transform\ Domain \rightarrow\ smaller\ \Delta x,\ higher\ resolution}$!

CHAPTER 4

EXPERIMENTAL METHODOLOGY

4.1 Structure proposed: Fourier Psychograph

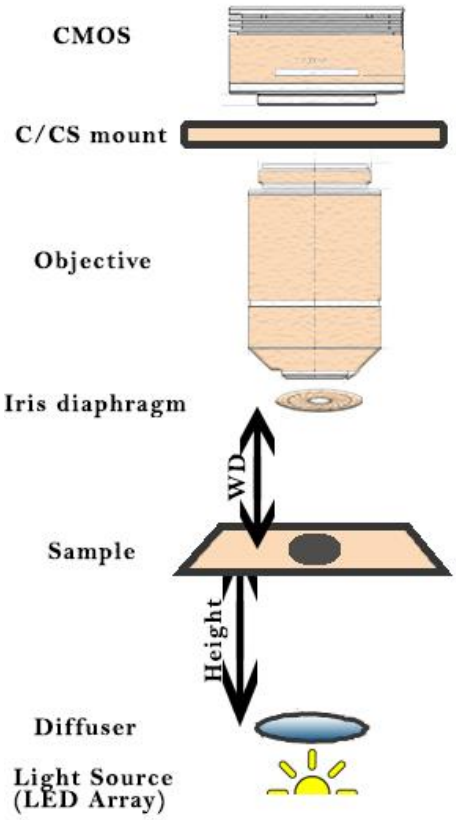

Computational Microscopy makes use of Fourier Ptychography technique.

The idea is to go through 4 iterative steps in order to reach the goal, as follows:

- Take a dataset of low-resolution images by turning ON the LED array indices one by one, thus obtaining one image for each LED index in the matrix.
- Define the centered image (illuminated from the LED index [16,16], the center of the matrix)
- Specify the angle of illumination, viewing angle and position of each image.
- Perform update in transform domain of the centered image, by adding information from the other low-resolution images.
- Result is a high-resolution image.

Now, since it is being used a LED array, it is need to make sure that when the cornered LED index is turned ON, its light will be reflected to the edge of the objective, thus being mirrored on CMOS. This detail is critical when defining relation Height-WD and choice of the Objective.

Computational Microscopy structure used

For the structure, the components have been altered with bought equipment referring to the paper analysis of previous microscopic structures. To test the computational microscopy scheme some components are added with their respective expectations: a) 32x32 RGB LED Array (Adafruit: ID 607, 50 EUR, to obtain a large dataset of max 1024 images), b) aperture (Edmund Optics: 53-907 & 57-574, 80 EUR, to increase contrast and depth of focus), c) light diffuser (Edmund Optics: 35-860 & 47-988, 139 EUR, to equally spread the light above the sample for better illumination), d) A. Basler acA4600-10uc (ID: 106538) Pixel size: 1.4um, Sensor size: 6.5 mm x 4.6 mm, color, 439 EUR.

4.2 Structure built: Fourier Ptychography

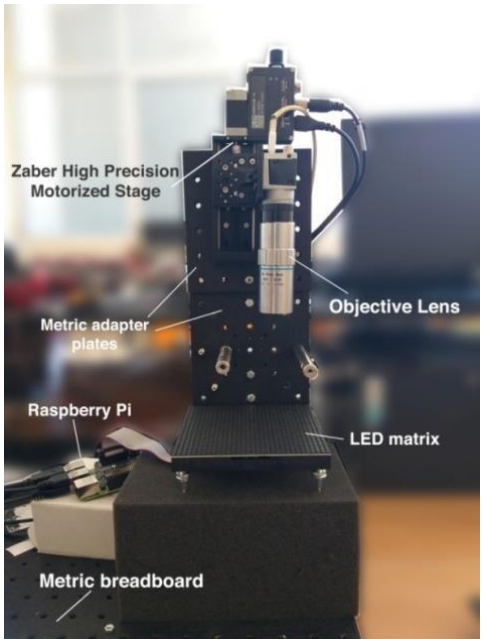

In the initially proposed Fourier Ptychography Microscopy system, LED array is used as an illumination source, where a single LED is turned on in each measurement.

As mentioned earlier LED array is placed sufficiently below the sample so that the illumination is considered to be spatially coherent. So in order to achieve this, the sample must be lifted at a fixed distance of few centimeters above the fixed LED matrix. This is done by means of metric adapter plates fixed on the metric breadboard using a 90° metric adapter that fits them together.

Figure 13 Structure proposed for experimental phase of refocusing

In order to perform the bright field refocusing that will correct for geometrical shifts and phase aberrations that degrade the resolution of the final image, the focus will be adjusted manually as proposed by using a step-controlled motor with high precision. The camera together with the lens is mounted to the Zaber stepper motor that is responsible for controlling the up and down movements of the sample each time the illumination angle hence the change of focus occurs. This motor is controlled by its own software while the LEDs are turned on sequentially by using a raspberry pi and a python script that identifies how the LEDs are turned on and the time slots for each of them being turned on. To obtain raw image data a CMOS sensor camera is used. It imposes a lot of advantages compared to CCD cameras where the most important one was the faster data acquisition rate. These cameras are also of lower cost compared to other cameras that may be used in modern digital microscopes.

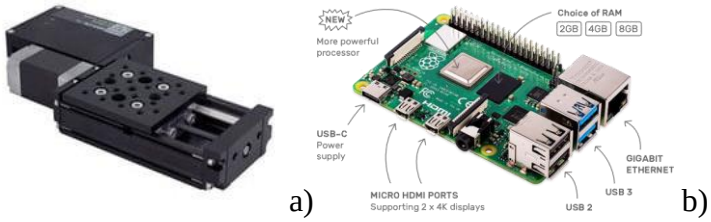

a) b)

Figure 14 a) Zaber step size motor and b) Raspberry Pi

4.3 Data acquisition methodology

The LED matrix in this setup is 32x32, however only a part of them is used to illuminate the specimen (5x5 and 10x10) as the other LEDs will produce a darkfield image which is not of the interest of what this thesis covers. The LED array is lifted with a block in order to obtain a distance of 6cm from the sample. This distance ensures an illumination that is spatially coherent so that the light emitted can be considered as a plane wave.

In order to light up a sufficient number of LEDs, Raspberry Pi is used. A python script is used to control the LED matrix by using loops that specify which LED should be turned on and the interval of time it spends in this condition [APPENDIX E]. The time is adjusted so that the specimen is not exposed for a long time in the light.

The pieces that are used to lift the structure are also from Edmund Optics. The CMOS camera from Basler is connected via a Micro A USB in order to achieve higher rate of data transmission. The software that is used to capture the raw images and view the specimen in real time is Pylon Viewer (Figure20) supplied by the same company as in CMOS camera. A step electric motor with high precision is used and is connected via a USB 3.0 to the computer. At its software the length scale of movement can be easily determined (minimum is order of 10-9 → nanometer) as well as the speed of movement, in case one is willing to automate the motion.

The dataset captured under the experiment conditions specified above use a rhizome cell and USAF 1951 Resolution Test chart. USAF is a standard component that is used mostly for optical instrument calibration and for resolution tests. It consists of some stripes of a specified length that are grouped in different numbers. To answer the question related to the effect of sample thickness in focus of the images, the USAF is placed between the two sides of a micro fluidic chamber with a considerable thickness of 4 mm each. To ensure better illumination intensity a box is used to block the room light interfering with the LED matrix.

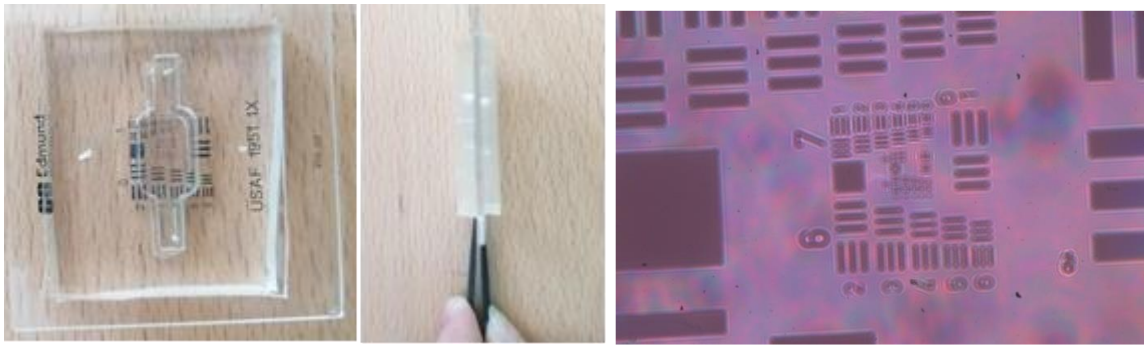

Figure 15 Micro fluidic chamber and USAF 1951 between the micro fluidic parts raw image

As it is stated at the previous section, it is needed to define an indexed angle for every LED illuminated, thus for every image acquired.

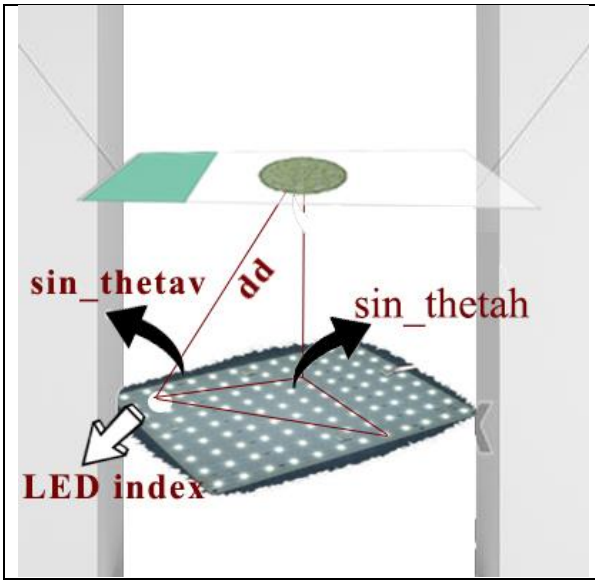

For every LED index, is defined an angle theta vertical and theta horizontal, which are used to project the image in the transform domain.

- dd represents the radius from the light source (respective LEDs) to the sample.
- Sin_thetav signifies the angle created from the radius and vertical catheter.
- Sin_thetah signifies the angle created from the Zero-position projection and the horizontal catheter.

When the code runs for a certain dataset, what we get is the reconstructed image of the centered image of the dataset. The dimensions of the reconstructed image are greater than those of the original one. Some of the raw images for each case are displayed below as follows.

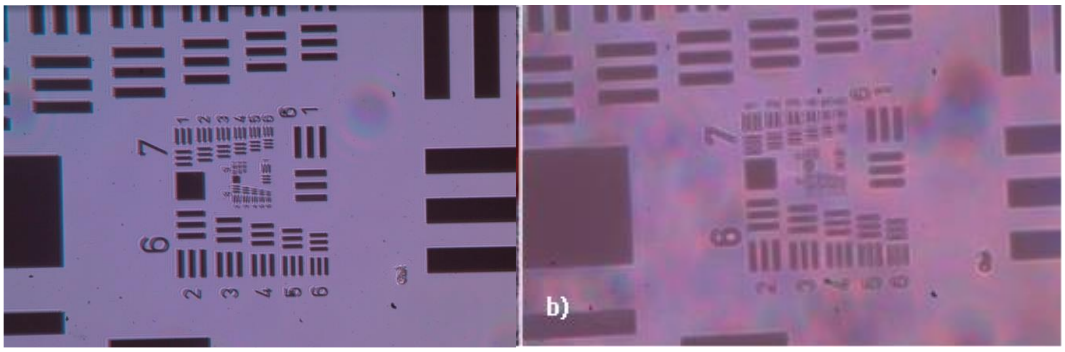

Figure 16 a) USAF 1951 raw image b) USAF 1951 between the micro fluidic parts raw image

6 different datasets were obtained:

1) 5x5 LEDs with USAF 1951 without refocusing, white light
2) 5x5 LEDs with USAF 1951 without refocusing, blue light
3) 5x5 LEDs with USAF 1951 without refocusing, green light
4) 5x5 LEDs with USAF 1951 without refocusing, red light
5) 5x5 LEDs with USAF 1951 with manual refocusing, white light
6) 10x10 LEDs with micro fluidic chamber without refocusing
7) Other datasets of Fern Ribozome cells and additional samples are kept in the lab book

4.4 Reconstruction process

This chapter addresses 2 of the hypothesis asked in the beginning of the thesis on what is the Fourier Ptychography microscopy dependent of. The first one is dependent on the optical path, how does it affect the quality of the final image if the adjustment is applied. The second one is dependent on the wavelength of the light source. Assuming the uncertainty principle, less information in x-space, more information in k-space. Blue light has a very low lambda compared to red light, which should result in higher information in k-space.

Both these hypotheses are experimentally observed and outputs are extracted from them.

4.4.1 All-in-focus dataset

The output of the algorithm is a reconstructed image with higher resolution, one image per each dataset. The details become more significant at the end of the preset number of iterations. The image with and without focus for each dataset are compared with each other by means of algorithms that calculate the contrast and the sharpness of each output.

Beginning with the first and second dataset '5x5 LEDs with USAF 1951 with and without refocusing', the synthesized numerical aperture of Fourier Psychograph is 0.9363 and the reconstructed image is displayed below together with the central raw image with maximum supposed intensity.

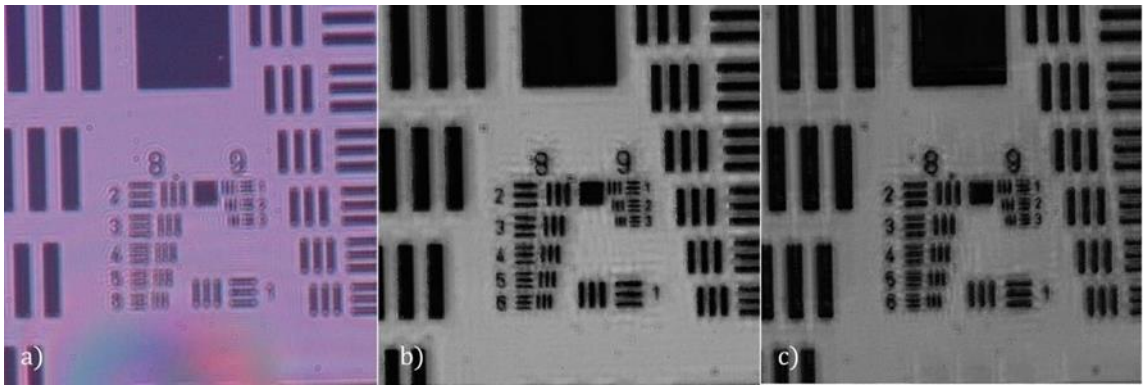

Figure 17 a) Raw image captured under central LED illumination b) Reconstructed image without applying the focus adjustment c) Reconstructed image with focus adjustment

With opinion - aware analysis one can deduce that the second image without using the method of refocusing appears to be sharper and preserve more details. However, by taking a look at the third image with the use of this method, even though the lines at Group 9 are not properly defined and separated from each other after the reconstruction process, the numbers

appear to be much more defined and sharper. This technique of active refocusing may be less robust to noise and therefore it cannot clearly separate the signal with important information from the estimated background noise. To sum up they both possess a high potential of providing the observer with more details than intended from raw image data that is collected.

The focus adjustment technique needs more improvement, such as determination of step size motion by another implemented algorithm.

To construct this algorithm one can obtain for example 10 raw images form an oblique illuminating plane wave by using a step of 0.1 micrometer for each image, and let another autofocus algorithm determine which of the obtained images is the best. By recording the step at each image, a path can be predicted that accounts for the adjustment of sample to objective distance, and implement this technique more accurately rather than opinion aware decision. This is left as a future work to anyone who would like to continue further.

a) 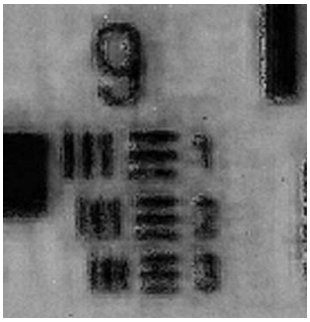 b) 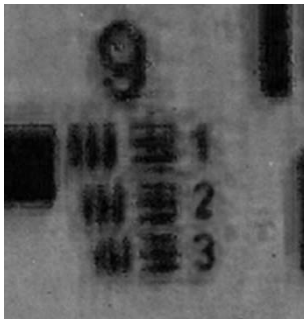

Figure 18 . a) Without refocusing b) With refocusing

Computational power is used to determine the image quality of both reconstructed images with the refocus method and without. The measured parameters are Brightness, Contrast, Sharpness, PIQE (Perception based Image Quality Evaluator) and NIQE (Natural Image Quality Evaluator). The respective values are displayed in Table below:

Table 3 Image Quality Measurement Parameters

	Brightness	**Contrast**	**Sharpness**	**PIQE**	**NIQE**
Raw Image	127.8978	86.5978	3.3886	6.1834	3.7108
Reconstructed Image without refocus	102.5594	86.5978	8.0382	26.8349	6.1941
Reconstructed Image with refocus	86.5976	86.5978	7.4473	26.1491	5.9478

Another important aspect of FPM is the effect of thickness, or the consideration of the third dimension of the sample. Since Fourier algorithm takes into account the slightest detail of the image, the angular illumination will cause some aberrations to the obtained data. Theoretically the glass specimen imposed an error to the data acquisition process of nearly 1 percent, which can or cannot be negligible. This depends in the application of FPM which is about slightest details in minute length scale. In case of micro fluidic chamber of thickness nearly 4 mm per each side, the error was very significant when compared to the same sample without the chambers. The thickness effect completely distorted the signal of the image, which was reconstructed with a not very pleasant resolution. So, this must also be taken into consideration when using different types of samples with varying thickness.

4.4.2 Different wavelength - light source

We have run the system (portable and inexpensive microscope) and we used to capture 4 datasets 5x5 (five by dive), which are; 5x5_white, 5x5_green, 5x5_blue, 5x5_red (the LED colors with different frequencies and wavelength). The aim is to provide the needed information to achieve the best result. During these trials we concluded that there are some environmental conditions that decreases our image quality. One of them is lack of darkness, because running the system in sunlight the contrast of our image lowers which leads us to lose sharpness of the image. We also run our system in a dark environment, which is easy to do so by using a box to cover microscope, we achieved better image quality, high and sharp contrast in black-white regions. These makes our sample easy to study and get all needed information from it.

Below I am showing the respective Datasets and the outputs that came from running the code in MATLAB, for each case I mentioned:

Dataset: 5x5_white light

While running the code for a certain dataset, what we expect to see is the reconstructed image of the centered image of the dataset. The dimensions of the reconstructed image are greater than those of the original one. In the first photo is shown the dataset we obtained by testing the sample with the white color. In this 2 images are shown the original and the reconstructed image that has resulted from the execution of codes in MATLAB. We can observe a slight difference in the resolution of the reconstructed image which is higher than the one of the original image and the reconstructed image is clearer and sharper.

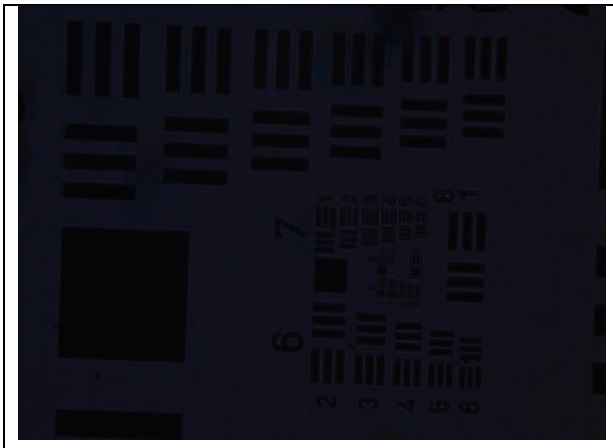

Figure 19 Original image captured by white light

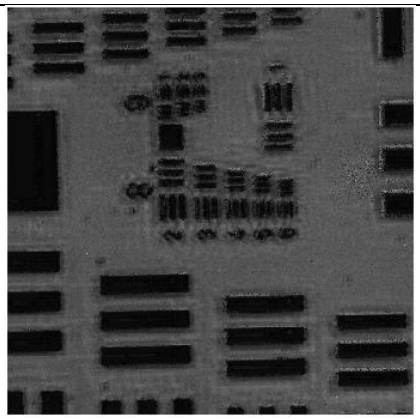

Figure 20 Reconstructed image captured by white light

Dataset: 5x5_red light

In the first photo is shown the dataset we obtained by testing the sample with the red color of the LED. As it is seen even in the original image the resolution is too low since during the experiment there was a lack of darkness, this way we expect the reconstructed image not to have the highest resolution possibly, but we can say that it's distinguishable.

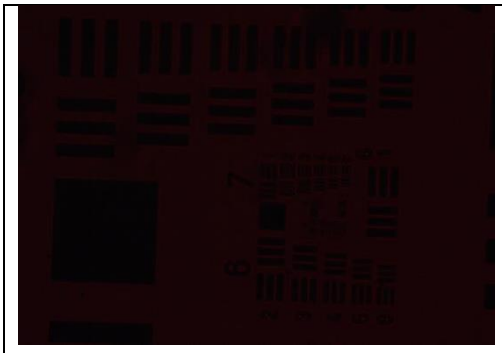

Figure 21 Original image captured by red light

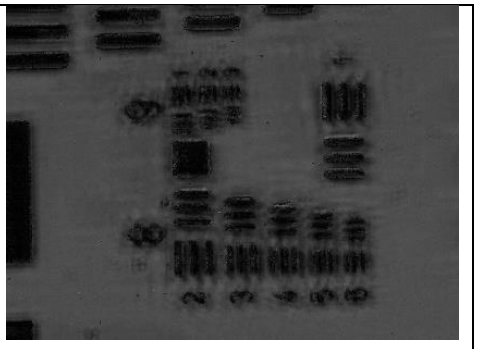

Figure 22 Reconstructed image captured by red light

Dataset: 5x5_green light

In the first photo is shown the dataset we obtained by testing the sample with the green color of the LED. In the second line of the image we can see the perfect Fourier results of amplitude and phase.

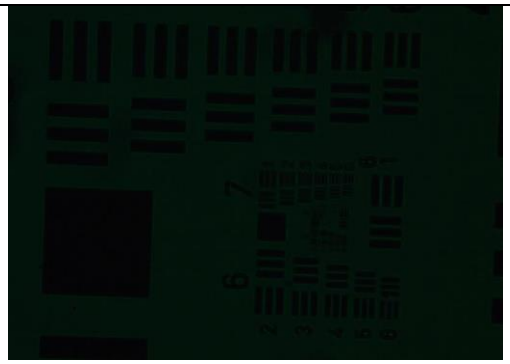

Figure 23 Original image captured by green light

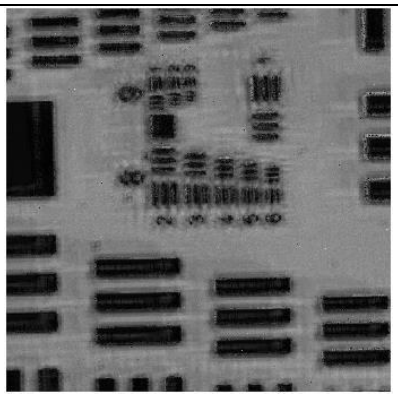

Figure 24 Reconstructed image captured by green light

Dataset: 5x5_blue light

In the first photo is shown the dataset we obtained by testing the sample with the blue color of the LED. In the second line of the image we can see the perfect Fourier results of amplitude and phase, in the first one in the phase is not projected to much information, but a difference in the resolution is evident in the image. We expect to see a better resolution in the reconstructed image comparing with the original one, since the wavelength of the blue light varies from 476.4nm +- 50nm.

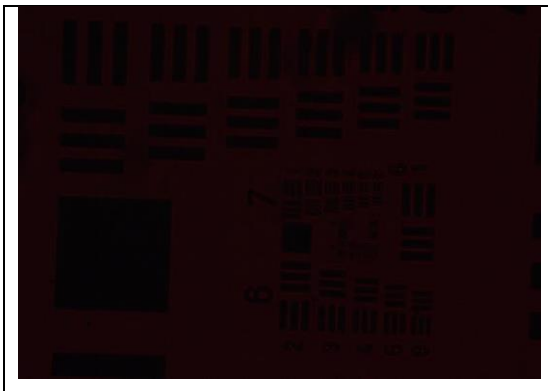

Figure 25 Original image captured by blue light

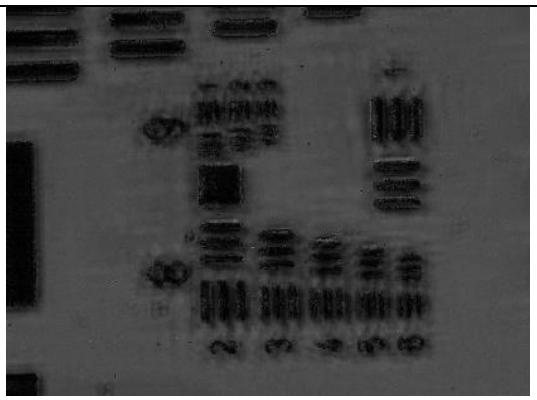

Figure 26 Reconstructed image captured by blue light

Comparative resulting

When all the reconstructed images are placed in a row for comparison, there is definitely observed a change in the process of reconstruction. The quality measurement for the current is undefined from more datasets needed to be taken in a more uniform background light so as to clearly see the interference patterns when reconstructed in different wavelength. For the moment it can be proved that the assumption is true, but if it increases the resolution or decreases it, is yet to be determined in a further experiment & analysis process.

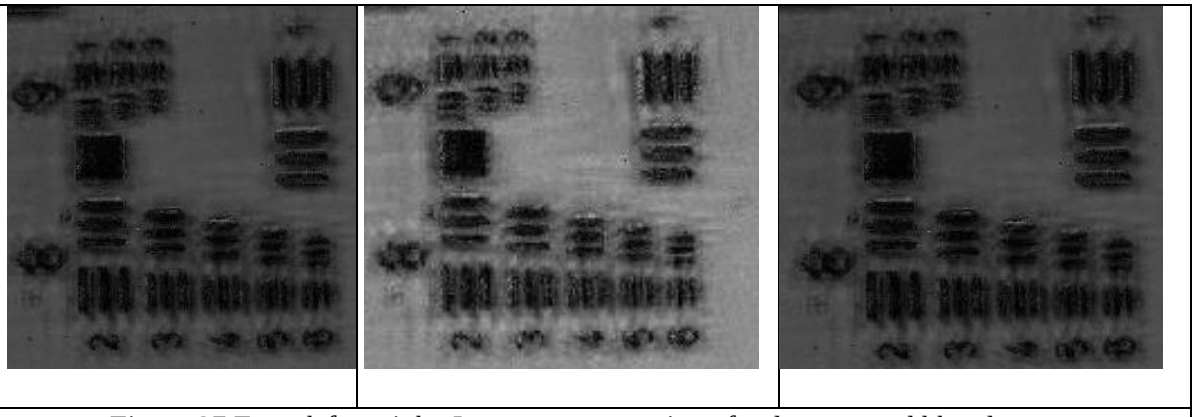

Figure 27 From left to right, Image reconstruction of red, green and blue dataset

4.5 Work timetable

Nb.	Logic Intervention	Duration	Description of activity
1.	Literature Review & Table of content (draft)	2 months	Gathering of papers and defining the methodology being experimented in current laboratories dedicated to the area of interest, critically thinking on the well-described methodology and pre-set hypothesis, based on expected results.
2.	"Dive into the device"	6 months	Weekly reports noted at the lab-book from experiments and observations, done with the equipment's found in the laboratory. Self-assembled portable microscope with all the parts being broken down to their unit function.
3.	Material ordering & tracking	6 purchase packages	Along the experiments, the need for an extra equipment arises sometimes, for biter adjustment. Contacting top companies in the field of optics & portable technologies (Edmund Optics[1], Throats[2], Digi key[3], Basler[4], Olympus, [5]Adafruit [6]etc.)
4.	Data Analysis & Algorithm testing	2 months	All datasets in Fourier Psychograph are subject to a computing algorithm which needs to be applied in order to visualize a high-quality output. Analysis on datasets taken and deep code understanding is done.

[1] https://www.edmundoptics.com/
[2] https://www.thorlabs.com/
[3] https://www.digikey.com/
[4] https://www.baslerweb.com/en/
[5] https://www.olympus-global.com/
[6] https://www.adafruit.com/

CHAPTER 5

FOURIER PTYCOGRAPHY USING LASER ARRAY

5.1 Prototyping scheme

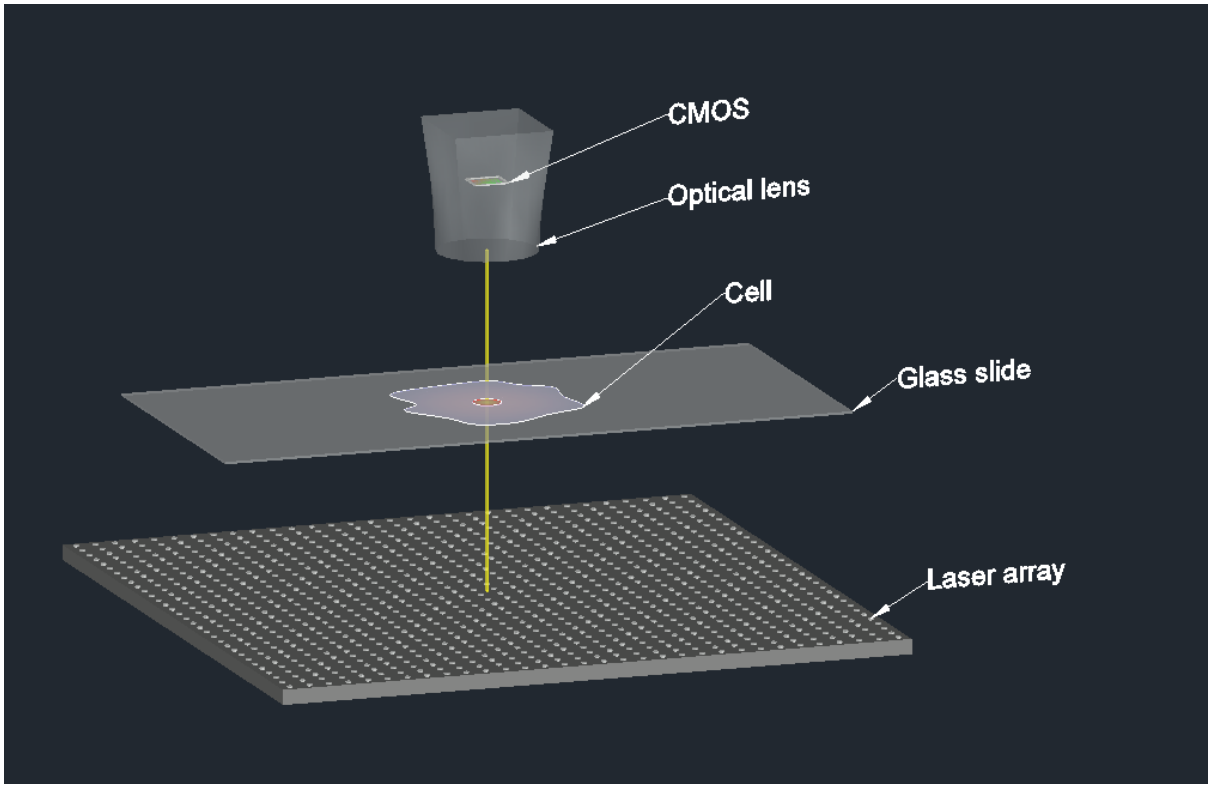

Figure 28 CAD Design of the portable microscope with programmable lighting

In Figure above, it is described how the prototype will look like and what are its main components. From the top, it will be purchased: a CMOS (camera, with pixel size 2.2 um) used to capture the image(s); Optical lens (light gathering system, consisting of objectives 20X, with working distance of minimum 10 mm); Glass slide and cells will be bought in stained mode for the sake of prototyping (later they will be taken from in-vitro organisms and be incubated to remain so during analysis); programmable units (raspberry PI and/or FPGA which allow to remotely run the program for image acquiring and analyzing, since they have their own computer chips). Laser array needs to be self-assembled since there is no company that offers it in the market. It can be done by purchasing the lasers through the support and after improvising a suitable “bed” for them with the help of a 3D printing device.

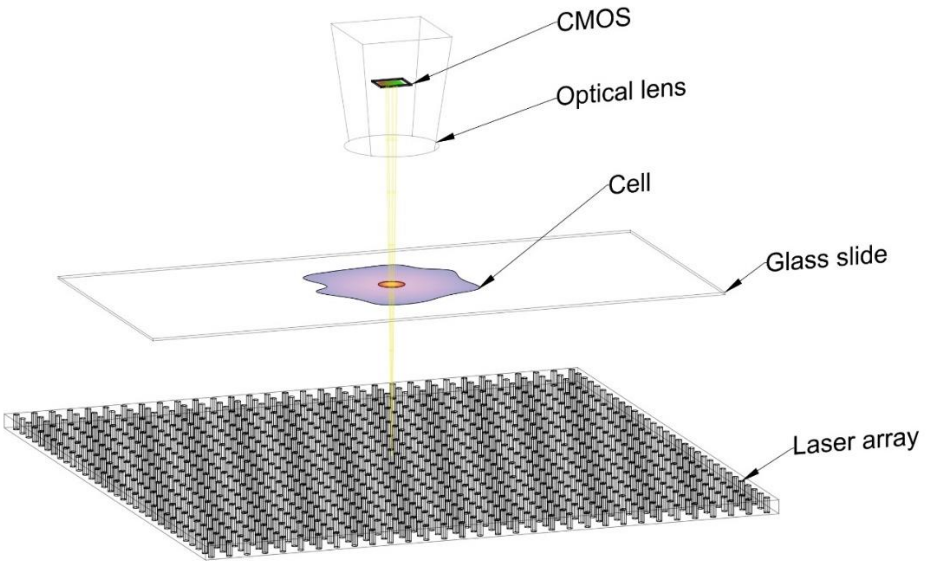

Figure 29 CAD Design of the light spreading and how the image is captured

With reference to Figure above, it can be explained that Fourier Psychograph aims to remove the barriers arising from physical limitations of the system. The ideology of using a light array instead of one single lighting point, is due to the light's wave nature, which scatters upon distance, by limiting the image acquired with most of the light focused on the center, and dimming towards the corners. Different light source will make it possible to cover all the region of the sample with sufficient lighting, thus giving a better image acquired at the end. The utilization of Laser instead of LED is to test the still-theoretical hypothesis, that the narrower bandwidth of Laser results in a higher spatial resolution after applying the reconstruction algorithms.

In concise form, to measure "the success" of our prototype, we aim to test and validate:

1. Test the performance of the laser array and optimise the spacing between lasers and their position.
2. Compare with results with LEDs to see if the image is better (contrast and resolution).

For quantitative evaluation of the performance of the microscope a magnifier tester will be used (for example like USAF1951). Software – adjust for the index of refraction for a living sample.

There is no company that offers a Light array with higher frequency resolution than LED's. We will have to manufacture it ourselves, or initially use a single light source that moves in steps of 4 mm in x-y plane.

5.2 Experiments and Discussions

5.2.1 Data acquisition methodology

To apply the experiment presented using Fourier Ptychography with laser as a light source illumination, we introduce a setup consisting of several components as illustrated in Figure 6. The components needed for this experiment are:

1. CMOS Basler acA4600 - 10uc (22896773)
2. Objective Mitutoyo 378-805-3 - M Plan Apo - 50x / 0.55 - ∞/ 0 - f = 200
3. Laser illumination (Green 532nm wavelength and Red 638 nm)
4. 40o diffuser
5. USAF target/ specimen
6. Zaber step motor (optional)
7. Metric adapters stages and optical table.
8. Microfluidic chambers

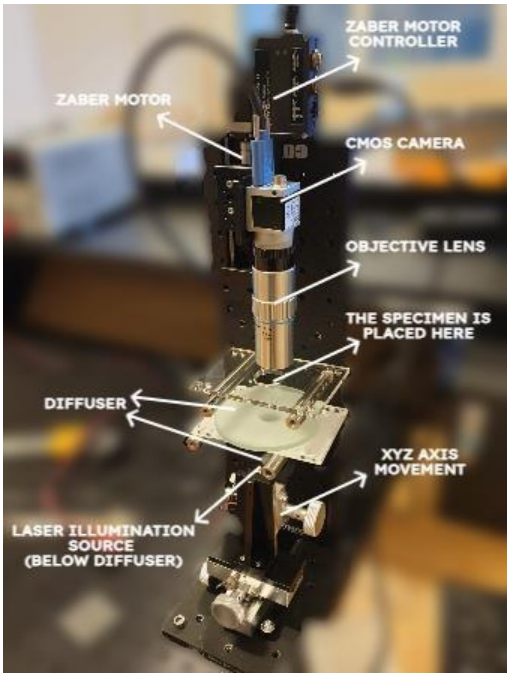

Figure 30 The setup constructed to obtain the images used as the dataset of this thesis

The structure is constructed using the supporting metric adapter stages and moving axis on top of an optical table. The whole structure height is 403 mm.

At the bottom of the structure is the laser source. The lasers used for this experiment are the green laser with 532 nm wavelength and the red laser with 638nm wavelength. The usage of two different lasers is for comparison reasons. On top of the laser is the diffuser with a 40o angle of diffraction.

At the distance of 50 mm away from the light source the specimen is placed. The distance from the optical table to the specimen is 216 mm. The optical lens is 13 mm away from the surface of the specimen. The height of the actual specimen should be considered as well, such that the working distance is always 13 mm for the specimen to be in focus.

The CMOS camera has a surface of 4608 (height) x 3288 (width) px, with each pixel being 1.4 x 1.4 μm, and a frame rate of 10fps. The Zaber motor in this case is optional, however for the CMOS camera to be placed at the exact distance from the specimen with nanometric accuracy, this kind of motor is needed. The Zaber motor makes possible the displacement of the camera together with the lens in one of the axes.

5.2.2 Reconstruction process

In the upcoming sections, we record and report the repercussions of using laser sources with different wavelengths in the conduction of the experiments. The information gathered is due to the illumination of the green laser (532 nm) and the red laser (638 nm). The results are analyzed based on the images obtained, and their corresponding values in terms of quality, image sharpness, contrast, etc.

As the next step in data acquisition, we make use of both green and red laser to obtain a matrix needed for the Fourier Ptychography and discuss how the use of laser gives results in terms of compatibility with the demand for good quality images. Moreover, the discussion is extended in the optimization of the laser as a source for Fourier Ptychography illumination.

Laser illumination using green 532 nm wavelength

Below we describe the process followed to obtain images using a green laser with 532 nm wavelength, the problems we faced and our solution on how to overcome these problems in order to optimize the quality of the images obtained using laser illumination as a source. We did this using an experimental technique rather than a computational one. The experiment set up explained in chapter 4 comprehends the process of projecting the light that falls on the specimen on the CMOS camera. The lens attached to the CMOS should be 13 mm away from the observed object, to obtain the best result possible in terms of focus.

For the analysis to be complete we conducted several experiments with the same specimen, but in different conditions. In the first run, we illuminated the sample placed in the focus distance from the lens directly without any diffuser. In Figure 8 is represented the image obtained:

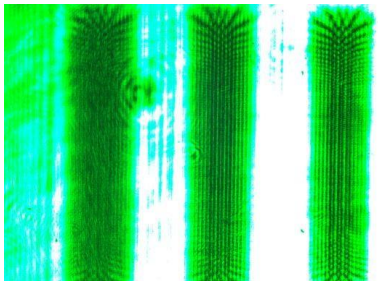

Figure 31 Image of the USAF target captured 13mm away from the lens

Looking at the image with the naked eye, the human perception of the quality can tell that this is not of the best quality, because of the lack of clarity. This means that the image components are difficult to distinguish. Analyzing the image shows that the contrast is high in

certain regions but low in others due to the differences in the light intensity from region to region. The seen disruptors in the image are the speckles of the laser introduced because of the spatial and temporal coherence of the laser beam that is projected onto the specimen. Laser speckle is a random phenomenon that can only be quantitatively characterized. Coherence of the laser comprises spatial resolution, which means that at a given moment in time, all points perpendicular to the laser beam in the same plane are in the same phase state, so they have the same EM value and direction.

The next step to improving the image quality was to try to uniformize the beam that is projected onto the sample. To achieve this task, we placed a static 40o diffuser between the laser source and the sample. The image shown below is the result of this approach.

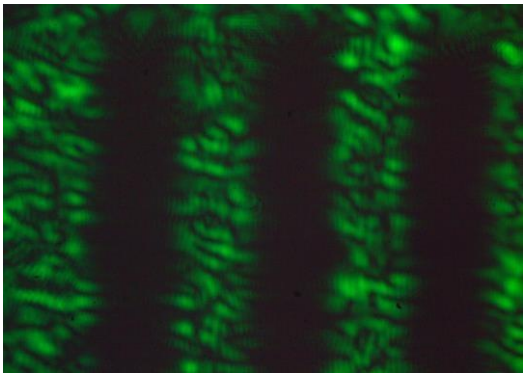

Figure 32 Image of the USAF target captured 13mm away from the lens, with a static diffuser between illumination source and the sample

This approach resulted in an image with a lower contrast level. The percentage of the contrast of the image taken without a diffuser to that taken with a static diffuser consists in a decrease of ~56% **[Table below]**. In contrary to the expected result, this image includes more speckles into the image. This image is harder for the human eye to distinguish, and as such is not considered as an acceptable result, as to what the FP with laser as illumination source tries to achieve.

We tried giving a solution to this problem using yet another diffuser. This time the diffuser is not static, but it is rotating with a constant angular velocity. This approach aims to decrease the presence of the speckles in the obtained images. Mathematically the speckles, which are variations of the light beam at certain zones, are averaged so the roughness is distributed, and the image appears smoother. In addition to the structure used before, a diffuser with a 40o angle of distribution is mounted into a motor using magnets. Different voltages are then applied to the motor to obtain variations in the angular velocity. When using

the **Mitutoyo** lens, the working distance is **13mm**. The diffuser is positioned **10mm** above the surface of the illumination source (green laser). When the motor is connected to a voltage source of 2.1 V and current 0.11A, the diffuser rotates with an angular velocity of 50.26 rad/s.

Figure 33 The motor and the diffuser used to realize the rotating diffuser

The method explained made possible capture of the following image:

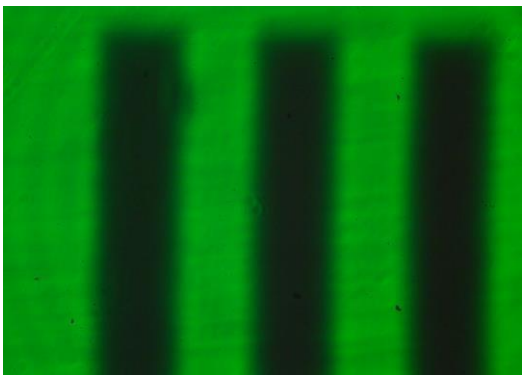

Figure 34 Image obtained using green laser as illumination source and a rotating diffuser with a constant angular velocity 50.2654824 rad/s

Perceived by the human eye, there is an improvement in the details of the image. Clearly, the bars in the image are easily distinguishable. This is due to averaging of the laser speckles (ripples) that are formed due to the coherence of the laser scattered from different parts of the illuminated sample. The presence of the diffuser diffracts the coherent light waves of the laser, which combined with the laser speckles result in blurry edges in the bars without much contrast. When rotating the diffuser, as explained above we obtain a better image in terms of detail discern. Since the rotation of the diffuser realizes the averaging of the intensities of the scattered illumination beams, it impacts the contrast and the sharpness of the image. Even though the image looks better in general, it will have lower scores in terms of contrast and sharpness.

Table illustrated below, has as its attributes the sharpness, contrast of the image, NIQE, and PIQE. The last two methods are MATLAB functions to determine the naturalness of the image and perceptual quality respectively. For the obtained images when applying different voltages to the rotating motor to obtain different angular velocities, we get the following results:

Table 4 MATLAB results for the naturalness of the image and quality, green laser

Voltage applied to the motor	Sharpness level	Contrast level	NIQE	PIQE
1.8	3.1271	134	4.8028	9.5915
1.9	3.1182	132	4.8265	9.6179
2.0	3.148	132	4.8487	9.9250
2.1	3.2179	135	4.8657	10.7778
2.2	3.2179	137	4.8699	10.5536
2.3	3.1412	139	4.8463	9.8329
Static Diffuser	4.5577	105	6.1752	22.9718
No Diffuser	6.264	241	4.1904	32.0855

The lowest the NIQE score, the better the naturalness of the image is. As for the PIQE, it is inversely correlated to the perceptual quality of an image. A low score value indicates high perceptual quality and a high score value indicates low perceptual quality.

Laser illumination using red 658 nm wavelength

The setup of this experiment is the same as the experiment done before using the green laser. For this experiment, we make use of a red laser as an illumination source to light the sample. To study the effect of the microfluidic chamber in which living cells are placed to be observed, we replicate the same conditions by placing the USAF 1951 target between two parts of a microfluidic chamber, for the diffraction of light from the material of the fluid chamber to be studied. In this experiment there are several images taken, each image differing from the other by changing the conditions to analyze their impact on the resolution and quality of the image. The first image taken is with the laser light that touches the sample directly without a diffuser between the specimen and the laser. The resulting image is given in Figure below.

Figure 35 Image with red laser illumination without a diffuser

As introduced before, to remove the speckles of the laser caused by the coherence of the light, we place a diffuser between the light source and the specimen, and we move the diffuser in the direction parallel to the plane of the placement of the specimen with a frequency of 5rot/min. The obtained image is shown below:

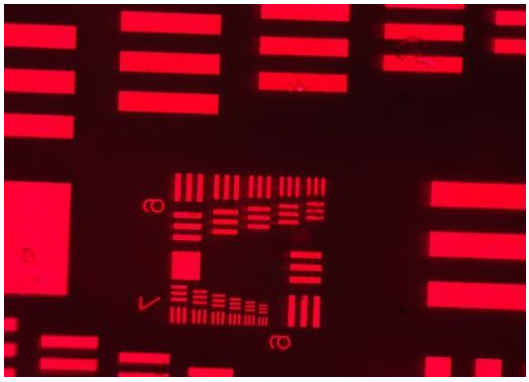

Figure 36 Image of the USAF 1951 with red laser illumination and moving diffuser

The images we obtained in this experiment using a red laser, are processed in MATLAB. For this experiment apart from the sharpness, contrast level, Niqe and Piqe another figure of merit for image quality assessment is used. Brisque which is a predefined function in MATLAB gives a calculation of the no-reference image quality score using the Blind/Referenceless Image Spatial Quality Evaluator. A smaller score in this case indicates better perceptual quality.

Table 5 MATLAB results for the naturalness of the image and quality, red laser

Image	Sharpness level	Contrast level	NIQE	PIQE	BRISQUE
Red Laser Without the diffuser	4.5901	241	3.6167	11.9396	7.1491
Red Laser with diffuser and moving	3.1549	111	5.2511	7.3790	30.1557
Red Laser Fluidic chamber without a diffuser	2.6998	103	5.5395	3.8028	37.0938
Red Laser Fluidic chamber static diffuser	4.5882	103	3.9959	4.2268	36.8657
Red Laser Fluidic chamber with moving diffuser	2.5579	80	6.2645	3.6800	33.2244

The data presented in Table 3 is to show the differences in images captured using two distinct laser wavelengths. The sharpness level for both images captured, without a diffuser and moving diffuser are of higher values for green laser. This result shows the superiority of the shorter wavelength when used to illuminate the source.

Table 6 Summary table for red and green lasers for naturalness of the image

Image	Sharpness level	Contrast level	NIQE	PIQE	BRISQUE
Red Laser Without a diffuser	4.5901	241	3.6167	11.9396	7.1491
No Diffuser	6.264	241	4.1904	32.0855	--
Red Laser Fluidic chamber with moving diffuser	2.5579	80	6.2645	3.6800	33.2244
Green Laser and Rotating Diffuser	3.2179	137	4.8699	10.5536	--

5.2.3 Observations & Results

The following experiment is conducted using both a green and a red laser (638nm wavelength) as an illumination source. The light from the laser is again projected onto the CMOS that is connected to the computer using a USB 3.0 to USB micro-B. The computer uses Pylon viewer as the software to obtain images from the connected Basler CMOS camera. We make use of the Zaber step motor to find the depth of the focus region of the camera accurately to nanometer scale. The Zaber step motor is connected to the computer using a USB 3.0 cable. The software used to control the zaber step motor is Zaber console.

The images are obtained sequentially, by turning on one of the lasers in the matrix and obtaining the image, then the other one, and so on in a predefined manner. There are three datasets acquired for this experiment. There is a green laser matrix dataset obtained by moving the diffuser. Another one by moving the diffuser and having the sample between the microfluidic chamber walls. The other data matrix obtained uses a red laser with the USAF 1951 target between microfluidic walls, obtained with a moving diffuser as well. The outputs of these datasets will be compared together to give an overview of the impact of the wavelength on the quality of the final image. Using a microfluidic chamber can introduce diffraction in the pattern of the light.

The microfluidic chamber provides a facile platform for studying cells. The chamber is fabricated using soft lithography, resulting in reproducible and high-throughput experiments. The reason why we made this choice is to create the conditions as near as possible, to how a living cell would be placed to be observed under the microscope. In this manner, we perceive the role in the diffraction of light of the material that makes up a microfluidic chamber, as well as its impact on the resolution or the quality of the image. We do not gather plenty of data that would give redundant information, as the data that is provided here is enough to give answers to the questions raised.

To obtain the reconstructed images of the datasets, we make use of the MATLAB code algorithm by Lei Tian. However before doing that we need to crop the images to size 2000 x 2000 px so the algorithm can run smoothly. To achieve this objective, we use the MATLAB code created. Having cropped the images to the right dimensions, we input the system setup parameters that correspond to the parameters we defined experimentally such as wavelength, numerical aperture, the distance between lasers, magnitude level, etc. (Found in the code).

With these steps done, we input the matrices one by one to the reconstruction algorithm and we obtain the data found in Figures below, by comparing them.

The difference is certainly distinguishable. The best results are taken when using the green laser as illumination source as the details are clearly visible. We can distinguish precisely group 8 and group 9, as well as each of the elements in these groups. The application of the microfluidic chamber does not show a negative impact on the final image. On the contrary, the details can be better than when not using it. This may be because of the material used to make these chambers diffract the laser light uniformly, thus behaving like a third "diffuser". When using red laser to illuminate the sample the obtained image is distorted to some extent. Even though we can distinguish some elements in group 8, the quality is bad.

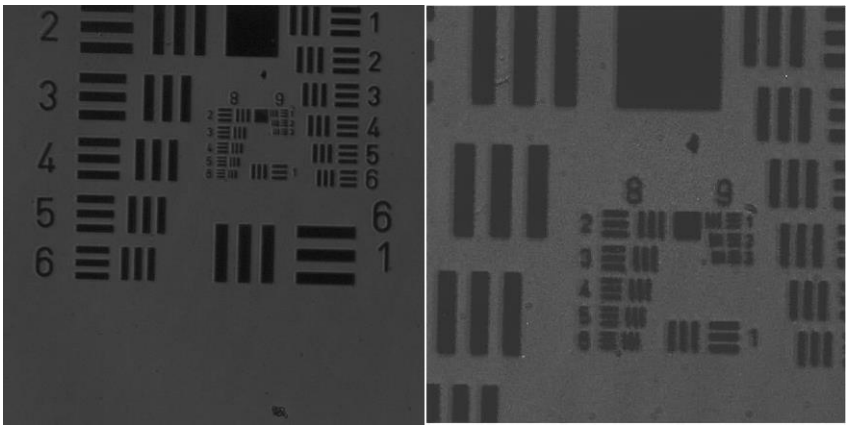

Figure 37 Green Laser and moving diffuser: Original Image & Reconstructed image

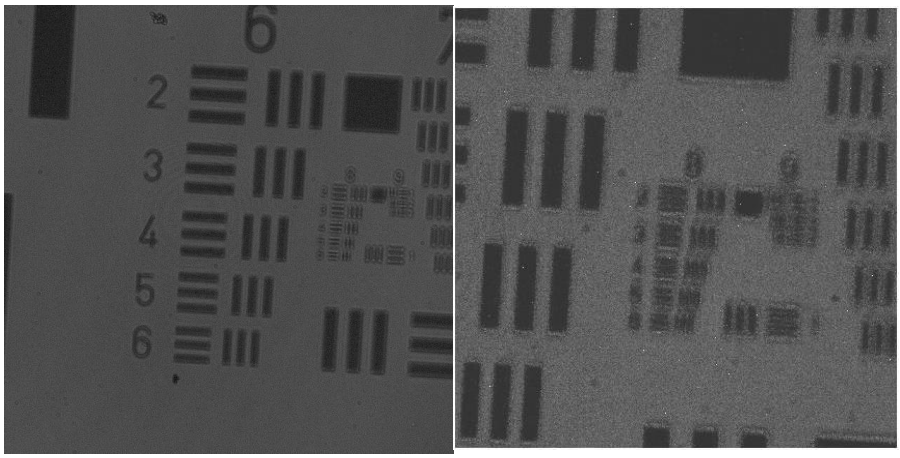

Figure 38 Red Laser and moving diffuser: Original Image & Reconstructed image

5.2.4 Perspective and Impact

First and foremost, to give a general overview of the impact that the illumination wavelength has on the quality of the image, more than two different light sources should be compared with each other. The blue and other EM spectrum colors should be used for this matter. There should also be work done in the enhancement of the FPM algorithm. High-speed cameras and high-speed laser matrix construction could lead to a new window for the FPM technique as it can give a real-time image assessment and correction, which could be applied in different fields such as medicine or medical imaging. This could be followed with the introduction of deep learning and neural network algorithms that will make possible artificial intelligence detection of image targets and faster FPM image reconstruction procedures.

This thesis could be seen as a starting point for new research on using different lasers as an illumination source. It can also help as a guide on how to construct an FP microscope and help in obtaining the dataset needed for the thesis purpose. This thesis delivers important results which can be further studied and enhanced so that new microscope models can be used.

5.3 EU4TECH PoC: Prototyping

Scientists at Epoka University Albania are participating in a H2020 project to develop new microscope technology. The specific aim for the Albanian team is to improve existing spatial resolution by supplying a portable microscope with hardware that allows for programmable lighting. This permits the use of image reconstruction algorithms to further improve the resolution. The platform under development will integrate not only the image acquisition (the microscope taking an image) but also the software that analyzes the images.

The EU4TECH PoC project will support the H2020 Eopka team to formulate a strong IPR strategy (C3) that will balance the requirement to publish with the need to secure IPR for commercialisation and to understand the market dynamics (C4), and how to develop in the Western Balkan settings (C5).

In the months to come, EU4TECH is supporting the Albanian team with some equipment bying with the aim of test-proofing ofthe ideology of narrow-bandwidth light source tobbe integrated in Fourier Ptychography Microscopy.

CHAPTER 6

FTIR SPECTROSCOPY IN BIOLOGICAL SAMPLES

6.1 FTIR-ATR

IR spectroscopy is an excellent method for biological analyses. It enables the non-perturbative, label-free extraction of biochemical information and images toward diagnosis and the assessment of cell functionality. Although not strictly microscopy in the conventional sense, it allows the construction of images of tissue or cell architecture by the passing of spectral data through a variety of computational algorithms.

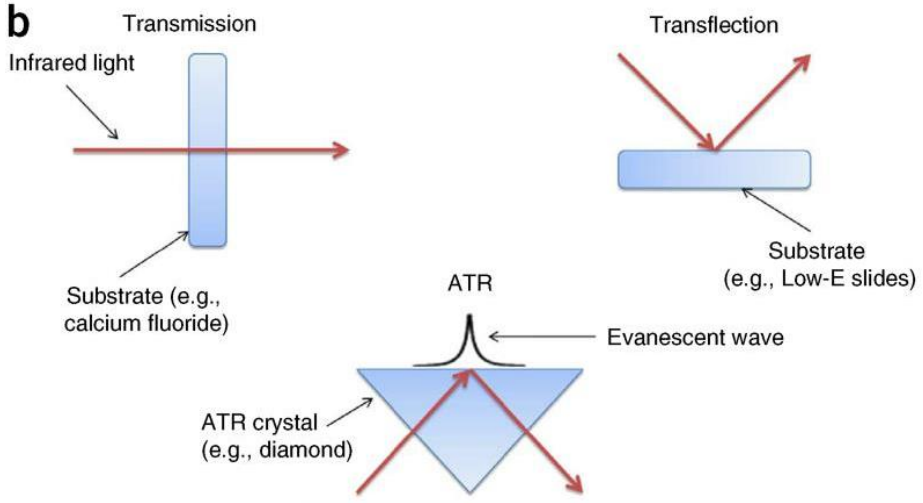

Figure 39 ATR, Transmission and Trans-reflection methods of FTIR

As described in the figure above, FTIR ATR is formed by sending a signal (infrared light beam) to the mirror, and letting the beam to propagate at the surface of the object under which it is placed. Then the signal with the obtained information will return to another mirror and be extracted its data collected. The process of 'beam hit' varies from 32 up to 64 beams, in order to find an average (best described) value of the data collected. The signal in the surface is called "evanescent wave", a travelling wave which registers through shifting on the object's surface. After acquisition, data processing consists of a sequence of steps including quality control, spectral pre-processing, feature extraction and classification of the supervised or unsupervised type. A typical

experiment can be completed and analysed within hours. Example results are presented on the use of IR spectra combined with multivariate data processing. [59]

PRO & CONS in Design

FTIR ATR & Transmission

Mode	**Suitable samples**	**Substrate**	**Typical interrogation area (µm)**
ATR	Tissues, cells and bio fluids	Calcium or barium fluoride, zinc selenide, MirrIR Low-E-coated glass	250 × 250
Transmission	Tissues, individual cells, cellular components and bio fluids	Calcium or barium fluoride and zinc selenide	5 × 5 to 150 × 150

Mode	**Pros**	**Cons**
ATR	-High SNR Reduced scattering -Analysis of large target area -Better for aqueous samples with appropriate substrate -Highest spatial resolution (because of the refractive index n, which is 3.5 or even 4 in case of Si or Ge)	Can be destructive because of pressure. Air between sample and IRE will affect spectra. Minimum sample thickness is required (~2.3 µm). Interactions of samples with the IRE leading to structural alterations (e.g., secondary protein structure).
Transmission	-High spatial resolution -Nondestructive of prepared sample -Automated stage allows for spectral acquisition at several different locations of choice with little user interaction	Lower SNR than ATR. Maximum sample thickness is required. Sample thickness should be twice as large as for transflection to achieve the same absorbance. Longer sample and machine preparation is required.

6.2 Methodology of Intervention

Based on the paper review, the scheme of how to analyse images taken from FTIR ATR[60] spectrum is described by the illustration below:

Wavenumber is the concept used in FTIR, and it is equal to $^1/_\lambda$, where λ is the wavelength of the infrared beam.

Since our spectrum varies from 4000 to 400 wavenumber (cm-1), then the wavelength of the Infrared beam varies from $^1/_{4000}$ to $^1/_{400}$ cm, or from 2.5 μm to 25 μm.

The graph can be represented by 4 categories, on what to expect from the curvatures shown in specific parts of the FTIR spectrum[61]. Based on the wavenumber values (cm-1)

- 4000 – 3500 -> It represents **the noise** of the wave
- 3500 – 2500 -> Here the curves determine **single bonds** of the atomic components
- 2500 – 2000 -> Here the curves determine **triple bonds** of the atomic components
- 2000 – 1500 -> Here the curves determine **double bonds** of the atomic components
- 1500 – 400 -> It is called the **"Fingerprint"** area, which is unique for every element

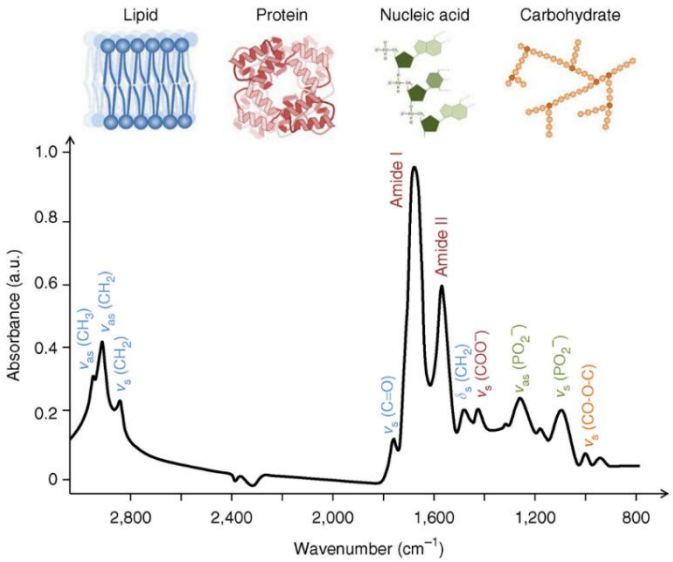

Figure 40 Typical biological spectrum showing bimolecular peak assignments from 3,000–800 cm−1,

6.3 Experiments and Data

FTIR ATR analysis was performed at the Institute of Nuclear Physics, in Albania. The device used operated by send an Infrared beam 62 times, and through its program, generates the mean graph with data from the evanescent wave on the object analysed. The graph shows the dependency of Transmittance to wavenumber (cm-1). The work with FTIR ATR has been developed in a chronological order, stated below:

- Spectrum of air has been registered (to remove the noise)
- Spectrum of the paper backgrounds have been taken (3 analyses for each paper)
- Spectrum of each ballpoint ink is registered in each paper (3 times for signature)

Table 7 Images of the analyzed spectrum of paper and signature

Paper analysis wth background air	**Ink analysis of the signature**
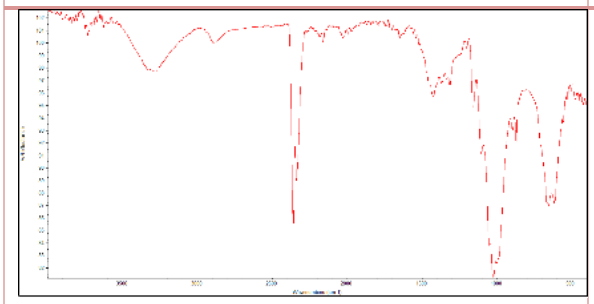	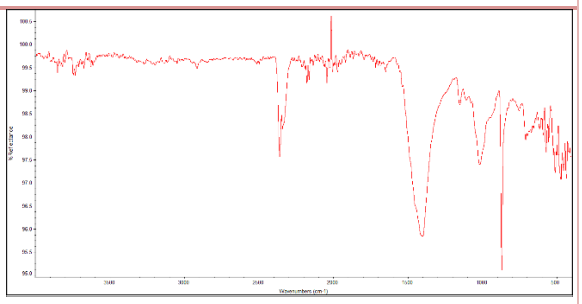
Figure 41 Spectrum of background of paper 1	*Figure 42 Spectrum of signature on paper 1*
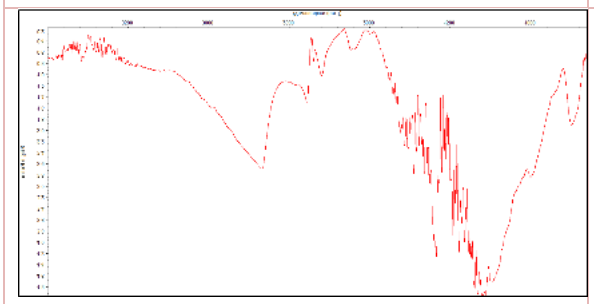	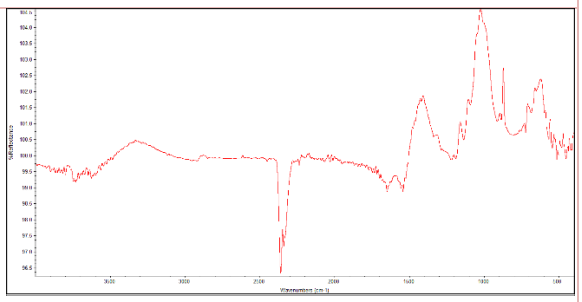
Figure 43 Spectrum of background of paper 2	*Figure 44 Spectrum of signature on paper 2*
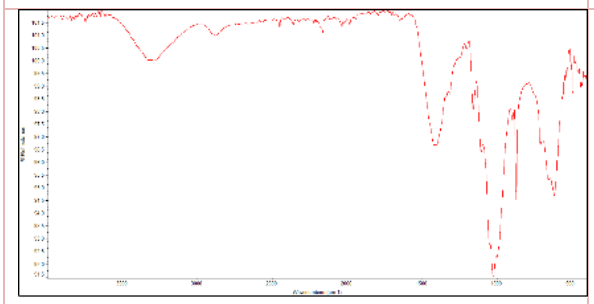	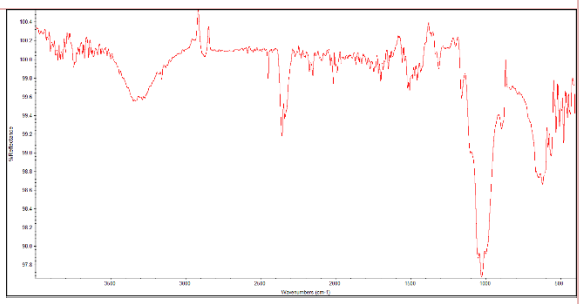
Figure 45 Spectrum of background of paper 3	*Figure 46 Spectrum of signature on paper 3*

6.4 Analysis for Polycarbonate material produced

Using FTIR ATR, we analyzed a sample created in laboratory conditions at EPOKA University. By using the Electro Spinner device, a material composed of mainly polycarbonate was produced. This material became sample at FTIR device, by giving the following spectrum, in relation Absorbance Vs Wavenumber.

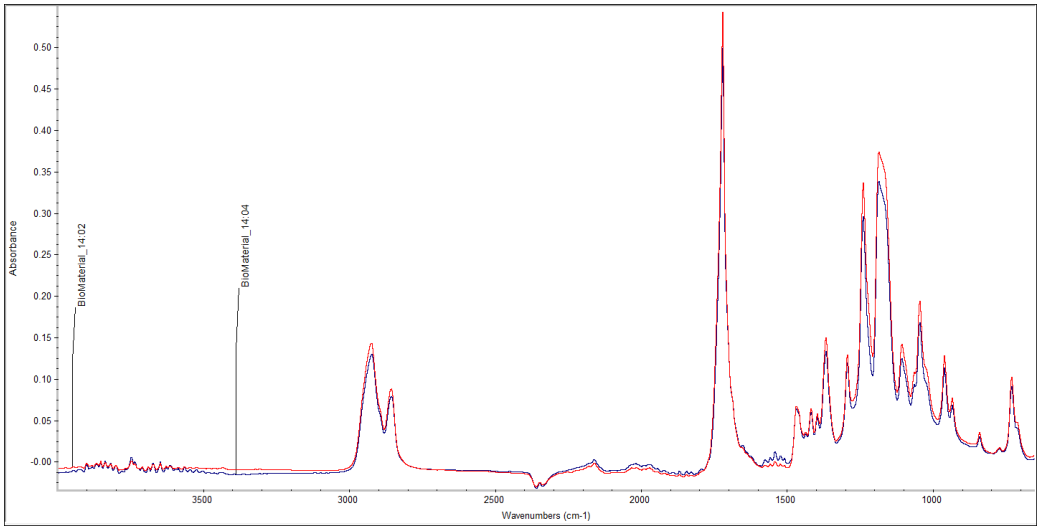

Figure 47 Spectrums of Polycarbonate material, in 2 minutes time distance

At the picture illustrated above, two times 64 infrared beams have passed at the surface of the biomaterial by giving the respective graphs (the red graph has been recorded at 14:02 PM and the blue graph has been recorded at 14:04 PM). Having a difference in time between each other was left intentionally. Since the graph is almost the same, we can say that this material doesn't evaporate and it is a well behavior-reproduction of a biomaterial.

From these graphs, two results emerge to be discussed:

- After subtracting the noise from the air by using the spectrum recorded of the air, we obtain the following graphs with these characteristics:
    - The level of noise, found between 4000 – 3500 wavenumbers, is very low, resulting in a good record of data, which can be trusted.
    - From 3500 – 2500, we can see a concentration at the region 2900-2750 wavenumber, which indicates the presence of some proteins.
    - From 2500 – 2000, we have the absence of triple bond concentration.
    - At 1750 wavenumber, at $\lambda = 5.7$ μm, for the region 2000 – 1500, there is a significant amount of absorption from the material, indicating high concentration of double carbonic bonds. Also, the temperature of the system at these bonds is low, since the space-bandwidth [60] is tight (indicating that the atoms are moving uniformly.

CHAPTER 7

RESULTS AND DISCUSSIONS

7.1 Results and conclusions: FPM

The objective of FPM is to use computing methods to solve difficulties that occur as a consequence of a system's optics' physical limits, and more specifically, to increase the optical system's space-bandwidth product (SBP) through computational (digital) techniques. This imaging approach recovers an accurate high-resolution, high-SBP output picture by repeatedly stitching together a series of low-resolution images in Fourier space. It is feasible to convert a normal microscope into a high-resolution, wide-FOV microscope with a final SBP of approximation by adding a simple LED matrix lighting module and employing FPM's reconstruction method.

In the beginning of the thesis, there were 3 different hypotheses raised, which are discussed below upon their successful completion or necessary adaption.

Hypothesis #1:

◊ Portable microscopes are composed of vital parts which reduces the hardware components and still extract the necessary information from the sample being studied to be able to quantify it in high resolution through coded algorithms. By increasing the computational complexity, it can be artificially increased the physical limitations arising in microscopy. Re-focusing of the optical path increases the output resolution in an improved factor.

For this hypothesis was proposed a different approach to the increment of reconstructed image resolution, by adjusting the focus manually using a geometrical approach to solve the problem. The relevant concepts to the theoretical approach of the proposed solution were also explained. Theoretically the thesis proves to be successful, relying also in the computational power to resolve the adjustment of image resolution. The effect of refocusing became much clear during the data analysis process, where the refocused raw data managed to produce an image of a higher quality and resolution. The

manual adjustment was made step by step in order to carefully observe the change in the shape and 3D effect of each captured image. Even though it took a few minutes of adjustment for 25 images, the pattern of motion can be translated into an algorithm and run by the Zaber Console Software in order to perform the active refocusing in an automated way.

Hypothesis #2:

◊ FPM works better if the LED is replaced by a light source with narrower bandwidth, which would naturally increase the resolution of the image datasets, which when reconstructed would produce a higher precision in the output image.

The difference is certainly distinguishable. The best results are taken when using the green laser as illumination source as the details are clearly visible. We can distinguish precisely group 8 and group 9, as well as each of the elements in these groups. The application of the microfluidic chamber does not show a negative impact on the final image. On the contrary, the details can be better than when not using it. This may be because of the material used to make these chambers diffract the laser light uniformly, thus behaving like a third "diffuser". When using red laser to illuminate the sample the obtained image is distorted to some extent. Even though we can distinguish some elements in group 8, the quality is bad.

Hypothesis #3:

◊ FPM implemented in a portable microscope is dependent on the optical path length, which acquires to manually or automatically adjust the focus distance on every iteration in order to provide a higher quality image of the sample.

As results, derived from the experiments regarding Hypothesis 2, we can mention that the hardware device compositions, play an important role in determining an optimal monitoring of samples / biomaterials.

From the performed experiments for datasets, it is observed that with the change of the wavelength, also the output image is affected. Low wavelength means high frequency and high frequency means more information in k-space. The assumption may

remain still as a future work, because of the very dark image datasets taken for the colored LED, which does not allow for a quantitative measurement of the results and their comparison. On the other hand, from all the performed experiments is seen that the resolution of the reconstructed image from datasets 5x5, 7x7, 9x9 is higher than the resolution of the original image and the resolution increase by increasing the number of images in the dataset. So as conclusion can be said that the resolution of the reconstructed image changes with the change of wavelength, which yet theoretically should be increasing and also it increases when the number of the images increases, but there should be well-defined the Noise from the surrounding environment. Further experiments need to be done to get a clear result.

7.2 Recommendations for future work

Fourier Ptychography Microscopy is the new era of digital medical imaging, where the use of computational provides a lot of advantages to its applications. This technique has not been mastered yet even though outstanding developments were made in the past decade. In such situation every contribution is essential.

Following the theoretical and experimental part of this thesis there is a lot of work to be done in order to achieve the best performance. Here will be discussed briefly the most common errors that directly affect the resolution of the reconstructed image.

- LED positioning – even after measurements and correct placing of the LED, it may not exactly lie at the position that is expected to. Self-calibration algorithms would solve such problem by correcting the imperfections of the alignment.

- LED intensity variation due to the different distances from the sample can be further corrected within the reconstruction process by measuring the brightness at the sample plane.

- Active focusing is in its early stages and still requires the expertise of biologists and scientists that can train the AI in the appropriate way.

- Failures may also arise from neglecting the effect of thickness of the sample. The reconstructed image may exhibit obvious aberrations such as non-uniform

surfaces causing the image to look like three dimensional, effects of immersion media, condensation of cover slips etc.

Several algorithms that correct for system parameters are now available and public, but most of them fix one error and cause one other. So, improvement of the Multiplexed Coded Illumination algorithm that accounts for robustness to noise and other aberrations correction has to be yet improved.

7.3 Thesis impact

Up to now, the thesis's work has been able to reach an audience of interested students, academic staff, entrepreneurs and other stakeholders, which have shown curiosity in either direct participation or being at the beneficiary side. The project is part of the prestigious accelerating program EU4TECH, funded by EU on a regional level (Western Balkans), where the Albanian team applied with the idea of MOHCI (Portable Microscopy employing Optimal Hardware and Computational Imaging). The idea started at the tier 3 of the Readiness project, to be accelerated through mentorship to tier 5-6: Prototype readiness and funding.

REFERENCES

[1] K. R. Spring and M. W, *Field of View*. .

[2] Bian; L.; Suo; J.; Dai; Q.; & Chen; F., "Fourier ptychography for high space- bandwidth product microscopy. Advanced Optical Technologies," 2017.

[3] A. Uka, A. Halili, X. Polisi, A. Osman Topal, G. Imeraj, and E. Vrana, "Basis of Image Analysis Methods for Cell Biomaterial Interaction," *Cells Tissues Organs*, 2021, doi: 10.1159/000512969.

[4] Lila, Stela and Uka, Arban, "A LAB BOOK TO DIGITAL IN LINE HOLOGRAHY: ALGORITHM NARRATION WITH EXPERIMENTAL ILLUSTRATIONS," EPOKA University, 2021.

[5] S. Rustemi and A. Uka, "Digital In-Line Holography: Main Applications and Methodology," EPOKA Unversity, 2020.

[6] L. Xeka and A. Uka, "CELL ANALYSIS USING BRIGHTFIELD AND PHASE CONTRAST MICROSCOPY," EPOKA University, 2019.

[7] I. Qose and A. Uka, "A lab book in Fourier Ptychographic Microscopy," EPOKA University, 2021.

[8] B. Shehu and A. Uka, "FOURIER PTYCHOGRAPHY ANALYSIS OF DATASETS PROBED WITH LASER ILLUMINATION IN VARYING LIGHT SPECTRUM," EPOKA University, 2021.

[9] B. Qesaraku and A. Uka, "EFFECT OF REFOCUSING IN FOURIER PTYCHOGRAPHIC MICROSCOPY," EPOKA University, 2021.

[10] "Depth of Focus, Olympus." [Online]. Available: https://www.olympus-ims.com/en/microscope/terms/.

[11] A. B. Vasista, D. K. Sharma, and G. V. P. Kumar, "Fourier Plane Optical Microscopy and Spectroscopy," *Digit. Encycl. Appl. Phys.*, pp. 1–14, 2019, doi: 10.1002/3527600434.eap817.

[12] "No Title." https://physicsworld.com/a/a-comprehensive-compendium-of-bioimaging-and-microscopy-technologies/.

[13] "No Title." https://www.youtube.com/watch?v=0aHVJW1dDUM.

[14] "No Title." https://scitechdaily.com/new-deep-learning-ai-tool-can-revolutionize-microscopy/.

[15] G. Zheng, R. Horstmeyer, and C. Yang, "Wide-field, high-resolution Fourier ptychographic microscopy," *Nat. Photonics*, vol. 7, no. 9, pp. 739–745, 2013, doi: 10.1038/nphoton.2013.187.

[16] K. Guo, S. Dong, and G. Zheng, "Fourier Ptychography for Brightfield, Phase, Darkfield, Reflective, Multi-Slice, and Fluorescence Imaging," *IEEE J. Sel. Top. Quantum Electron.*,

vol. 22, no. 4, pp. 77–88, Jul. 2016, doi: 10.1109/JSTQE.2015.2504514.

[17] L. Tian, X. Li, K. Ramchandran, and L. Waller, “Multiplexed coded illumination for Fourier Ptychography with an LED array microscope,” *Biomed. Opt. Express*, vol. 5, no. 7, p. 2376, 2014, doi: 10.1364/boe.5.002376.

[18] “No Title.” https://ist.ac.at/en/research/danzl-group/#Current Projects.

[19] D. Dominguez, N. Alharbi, M. Alhusain, A. A. Bernussi, and L. G. De Peralta, “Fourier plane imaging microscopy,” *J. Appl. Phys.*, vol. 116, no. 10, 2014, doi: 10.1063/1.4895157.

[20] O. N. A. Morel *et al.*, “Wide-field lensfree imaging of tissue slides,” *Opt. InfoBase Conf. Pap.*, no. September, 2014, doi: 10.1117/12.2183462.

[21] G. Imeraj and A. Uka, “OPTIMAL MONITORING OF BIOMATERIALS USING DIGITAL IN-LINE HOLOGRAPHIC MICROSCOPY,” EPOKA, 2019.

[22] B. Osgood, “EE261 - Fourier Transform and its applications,” *Lect. Notes EE 261 - Fourier Transform its Appl.*, pp. 26–33, 2014.

[23] M. Kellman, M. Chen, Z. F. Phillips, M. Lustig, and L. Waller, “Motion-resolved quantitative phase imaging,” *Biomed. Opt. Express*, vol. 9, no. 11, p. 5456, Nov. 2018, doi: 10.1364/BOE.9.005456.

[24] D. Lee, S. Ryu, U. Kim, D. Jung, and C. Joo, “Color-coded LED microscopy for multi-contrast and quantitative phase-gradient imaging,” *Biomed. Opt. Express*, vol. 6, no. 12, p. 4912, Dec. 2015, doi: 10.1364/BOE.6.004912.

[25] J. C. Ramella-Roman, Ed., “Polarized Light and Optical Angular Momentum for Biomedical Diagnostics,” 2021, p. 128 (1 Vol).

[26] “No Title.” https://focalplane.biologists.com/2021/04/28/compact-and-high-performance-fluorescence-microscopy/.

[27] “No Title.” https://phys.org/news/2020-05-laboratory-grade-microscope-us18.html.

[28] B. Diederich *et al.*, “A versatile and customizable low-cost 3D-printed open standard for microscopic imaging,” *Nat. Commun.*, vol. 11, no. 1, 2020, doi: 10.1038/s41467-020-19447-9.

[29] P. C. Konda, L. Loetgering, K. C. Zhou, S. Xu, A. R. Harvey, and R. Horstmeyer, “Fourier ptychography: current applications and future promises,” *Opt. Express*, vol. 28, no. 7, p. 9603, Mar. 2020, doi: 10.1364/OE.386168.

[30] P. C. Konda, J. M. Taylor, and A. R. Harvey, “High-resolution microscopy with low-resolution objectives: correcting phase aberrations in Fourier ptychography,” Sep. 2015, p. 96300X, doi: 10.1117/12.2191338.

[31] Y. S. Zhang *et al.*, “A cost-effective fluorescence mini-microscope for biomedical

applications," *Lab Chip*, vol. 15, no. 18, pp. 3661–3669, 2015, doi: 10.1039/c5lc00666j.

[32] S. B. Kim *et al.*, "A mini-microscope for in situ monitoring of cells.," *Lab Chip*, vol. 12, no. 20, pp. 3976–3982, 2012, doi: 10.1039/c2lc40345e.

[33] Y. S. Zhang, G. Trujillo-de Santiago, M. M. Alvarez, S. J. Schiff, E. S. Boyden, and A. Khademhosseini, "Expansion mini-microscopy: An enabling alternative in point-of-care diagnostics," *Curr. Opin. Biomed. Eng.*, vol. 1, pp. 45–53, 2017, doi: 10.1016/j.cobme.2017.03.001.

[34] Y. S. Zhang *et al.*, "Hybrid Microscopy: Enabling Inexpensive High-Performance Imaging through Combined Physical and Optical Magnifications," *Sci. Rep.*, vol. 6, no. November 2015, pp. 1–10, 2016, doi: 10.1038/srep22691.

[35] "No Title." https://hackaday.com/2020/03/11/getting-1000-fps-out-of-the-raspberry-pi-camera/.

[36] Z. F. Phillips, "Quantitative Microscopy using Coded Illumination," 2019.

[37] H. Lee, B. H. Chon, and H. K. Ahn, "Reflective Fourier ptychographic microscopy using a parabolic mirror," *Opt. Express*, vol. 27, no. 23, p. 34382, Nov. 2019, doi: 10.1364/OE.27.034382.

[38] M. Kellman, E. Bostan, M. Chen, and L. Waller, "Data-Driven Design for Fourier Ptychographic Microscopy," Apr. 2019, [Online]. Available: http://arxiv.org/abs/1904.04175.

[39] J. Sun, C. Zuo, J. Zhang, Y. Fan, and Q. Chen, "High-speed Fourier ptychographic microscopy based on programmable annular illuminations," *Sci. Rep.*, vol. 8, no. 1, pp. 1–3, 2018, doi: 10.1038/s41598-018-25797-8.

[40] L. Rong *et al.*, "Continuous-wave terahertz reflective ptychography by oblique illumination," *Opt. Lett.*, vol. 45, no. 16, p. 4412, 2020, doi: 10.1364/ol.400506.

[41] L. Valzania, E. Hack, P. Zolliker, R. Brönnimann, and T. Feurer, "Resolution limits of terahertz ptychography," no. May, p. 72, 2018, doi: 10.1117/12.2307157.

[42] A. E. Carpenter *et al.*, "CellProfiler: Image analysis software for identifying and quantifying cell phenotypes," *Genome Biol.*, vol. 7, no. 10, 2006, doi: 10.1186/gb-2006-7-10-r100.

[43] J. Isakovic, I. Dobbs-Dixon, D. Chaudhury, and D. Mitrecic, "Modeling of inhomogeneous electromagnetic fields in the nervous system: a novel paradigm in understanding cell interactions, disease etiology and therapy," *Sci. Rep.*, vol. 8, no. 1, pp. 1–20, 2018, doi: 10.1038/s41598-018-31054-9.

[44] J. Garbrecht *et al.*, "Simultaneous dual-channel imaging to quantify interdependent protein recruitment to laser-induced dna damage sites," *Nucleus*, vol. 9, no. 1, pp. 474–491, 2018, doi: 10.1080/19491034.2018.1516485.

[45] “No Title.” https://www.spiedigitallibrary.org/conference-proceedings-of-spie/10677/2307157/Resolution-limits-of-terahertz-ptychography/10.1117/12.2307157.full?SSO=1.

[46] X. Ou, R. Horstmeyer, G. Zheng, and C. Yang, “High numerical aperture Fourier ptychography: principle, implementation and characterization,” *Opt. Express*, vol. 23, no. 3, p. 3472, Feb. 2015, doi: 10.1364/OE.23.003472.

[47] J. C. Glover *et al.*, “In vivo Cell Tracking Using Non-invasive Imaging of Iron Oxide-Based Particles with Particular Relevance for Stem Cell-Based Treatments of Neurological and Cardiac Disease,” *Mol. Imaging Biol.*, vol. 22, no. 6, pp. 1469–1488, 2020, doi: 10.1007/s11307-019-01440-4.

[48] J. Sun, C. Zuo, J. Zhang, Y. Fan, and Q. Chen, “High-speed Fourier ptychographic microscopy based on programmable annular illuminations,” *Sci. Rep.*, vol. 8, no. 1, pp. 1–12, 2018, doi: 10.1038/s41598-018-25797-8.

[49] C. Zuo, J. Sun, and Q. Chen, “Adaptive step-size strategy for noise-robust Fourier ptychographic microscopy,” *Opt. Express*, vol. 24, no. 18, p. 20724, Sep. 2016, doi: 10.1364/OE.24.020724.

[50] C. Yang, J. Qian, A. Schirotzek, F. Maia, and S. Marchesini, “Iterative Algorithms for Ptychographic Phase Retrieval,” vol. 23, no. 12, pp. 12027–12038, 2011, [Online]. Available: http://arxiv.org/abs/1105.5628.

[51] A. Pan, Chao Zuo, Yuege Xie, Ming Lei, and Baoli Yao, “Vignetting effect in Fourier ptychographic microscopy,” *Opt. Lasers Eng.*, vol. 120, no. November 2018, pp. 40–48, 2019, doi: 10.1016/j.optlaseng.2019.02.015.

[52] R. Claveau, P. Manescu, M. Elmi, V. Pawar, M. Shaw, and D. Fernandez-Reyes, “Digital refocusing and extended depth of field reconstruction in Fourier ptychographic microscopy,” *Biomed. Opt. Express*, vol. 11, no. 1, p. 215, 2020, doi: 10.1364/boe.11.000215.

[53] Atul Kumar Verma, “Fourier Transform - A Visual Introduction.ipynb.” https://github.com/thatSaneKid/fourier/blob/master/Fourier Transform - A Visual Introduction.ipynb.

[54] M. Kellman, E. Bostan, M. Chen, and L. Waller, “Data-Driven Design for Fourier Ptychographic Microscopy,” *2019 IEEE Int. Conf. Comput. Photogr. ICCP 2019*, pp. 1–8, 2019, doi: 10.1109/ICCPHOT.2019.8747339.

[55] S. Dong, J. Liao, K. Guo, L. Bian, J. Suo, and G. Zheng, “Resolution doubling with a reduced number of image acquisitions,” *Biomed. Opt. Express*, vol. 6, no. 8, p. 2946, Aug. 2015, doi: 10.1364/BOE.6.002946.

[56] A. S. Vasilevich, A. Carlier, J. de Boer, and S. Singh, “How Not To Drown in Data: A Guide for Biomaterial Engineers,” *Trends Biotechnol.*, vol. 35, no. 8, pp. 743–755, Aug. 2017, doi: 10.1016/j.tibtech.2017.05.007.

[57] X. Ou, R. Horstmeyer, C. Yang, and G. Zheng, “Quantitative phase imaging via Fourier ptychographic microscopy,” *Opt. Lett.*, vol. 38, no. 22, p. 4845, Nov. 2013, doi: 10.1364/OL.38.004845.

[58] L. Tian and L. Waller, “3D intensity and phase imaging from light field measurements in an LED array microscope,” *Optica*, vol. 2, no. 2, p. 104, Feb. 2015, doi: 10.1364/OPTICA.2.000104.

[59] L. M. Ailioaie and G. Litscher, *Molecular and cellular mechanisms of arthritis in children and adults: New perspectives on applied photobiomodulation*, vol. 21, no. 18. 2020.

[60] A. W. Lohmann, R. G. Dorsch, D. Mendlovic, C. Ferreira, and Z. Zalevsky, “Space–bandwidth product of optical signals and systems,” *J. Opt. Soc. Am. A*, vol. 13, no. 3, p. 470, 1996, doi: 10.1364/josaa.13.000470.

[61] www.azom.com/article.aspx?ArticleID=12063. PIKE Technologies, “Using FTIR-ATR Spectroscopy to Rapidly Analyze Inks,” 2015, [Online]. Available: http://www.azom.com/article.aspx?ArticleID=12063.

APPENDIX A: Dataset Folders for FPM, DIHM, BF

- https://drive.google.com/drive/folders/1EJdsKJyTfw1GHQm6Asas_MRjhnm7qYEU?usp=sharing

APPENDIX B: Python Codes for Fourier Optics

- https://github.com/thatSaneKid/fourier/blob/master/Fourier%20Transform%20-%20A%20Visual%20Introduction.ipynb

```
import matplotlib
from matplotlib import pyplot as plt
import numpy as np
import seaborn as sns
sns.set()

f1 = 3.0
f2 = 5.0
t = np.arange(0,2,0.001)

cos_wave1 = np.cos(2*np.pi*f1*t)
cos_wave2 = np.cos(2*np.pi*f2*t)
cos_wave = cos_wave1+cos_wave2
# cos_wave = 2*m.cos(2*np.pi*f*t) + 5*m.cos(2*np.pi*f*2*t)

r_cord = []
min_freq_range = 1
max_freq_range = 9
sf_list = np.arange(min_freq_range, max_freq_range, 1)
for sf in sf_list:
    r_cord.append( [(cos_wave[i], t[i]*sf*2*np.pi) for i in range(len(t)) ] )

x_cord , y_cord = [], []
for l in range(len(r_cord)):
    x_cord.append( [amp*np.cos(theta) for (amp,theta) in r_cord[l]] )
    y_cord.append( [amp*np.sin(theta) for (amp,theta) in r_cord[l]] )

mean_list = []

plt.rcParams["figure.figsize"] = (15,110)
for l in range(len(r_cord)):
    plt.subplot(int(len(r_cord)/4)+1, 4, int(l+1))
    plt.plot(x_cord[l], y_cord[l])
    plt.plot(np.mean(x_cord[l]), np.mean(y_cord[l]), 'or' )
    plt.title("Sampling Freq = "+str(round(sf_list[l], 2))+" Hz")

    # Storing the COM for plotting later
    x_mean = np.sum(x_cord[l])
    mean_list.append(x_mean)

plt.show()
```

APPENDIX C: MATLAB code for FPM, Tian Lab

- https://github.com/Waller-Lab/FPM

APPENDIX D: MATLAB Code for automatic image crop

```
% By BESMIR SHEHU, bshehu18@epoka.edu.al
% FILE DIRECTORY TO GET THE IMAGES
filedir = ['./ORIGIN FILENAME/'];
% FOLDER WHERE THE IMAGES WILL BE STORED
out_dir = ['./RED Microfluidic 5x5'];
mkdir(out_dir);
% GET ALL THE IMAGES THAT END WITH THE FOLLOWING EXTENSION:
imglist = dir([filedir,'*.png']);
for m=1:length(imglist)
I = [filedir,imglist(m).name];
% NAME ALL IMAGES e.g. myimage1.png AS SHOWN BELOW:
baseFileName = sprintf('myimage%02d.png', m);
I = imread(I);
I=uint8(I);
% ENTER THE CROP SIZE
cropSize = [2000 2000];
r = centerCropWindow2d(size(I),cropSize);
J = imcrop(I,r);
fullFileName = fullfile(out_dir, baseFileName);
imwrite(J, fullFileName);
end
```

APPENDIX E: Python Script for Control of Led Matrix

```
from samplebase import SampleBase import time
class SimpleSquare(SampleBase):
def  init (self, *args, **kwargs): super(SimpleSquare, self). init (*args, **kwargs)
def run(self):

“creates a frame which later will be lighten up like creating a 2D array (matrix)” offset_canvas =
self.matrix.CreateFrameCanvas()
while True:

for y in range(13,20): “select number of rows which in this case are 7” for x in range(13,20): “select
number of colums which is also 7”
“set to 0 (off) all the leds if anyone is on” offset_canvas = self.matrix.CreateFrameCanvas()
“set the (x,y) pixel on which in led corresponds to x row and y column offset_canvas.SetPixel(x, y, 255, 0,
0)
“turn on (x,y) led on led matric pannel
offset_canvas = self.matrix.SwapOnVSync(offset_canvas) “Wait one seconed before repeating the steps”
time.sleep(1)
“ set all the leds to 0 (off)”
offset_canvas = self.matrix.CreateFrameCanvas() offset_canvas =
self.matrix.SwapOnVSync(offset_canvas) break
# Main function
if    name           == " main ": simple_square = SimpleSquare() if (not simple_square.process()):
simple_square.print_help()
```

APPENDIX F: Pricing of Components from Purchase Orders

Component name	Company	Price	Part Number
50X Mitutoyo Plan Apo Infinity Corrected Long WD Objective	Edmund Optics	$2650.00	#46-146
Zaber™ High Precision Motorized Stage Systems	Edmund Optics	$1850.00	#15-286
Metric Breadboard	Edmund Optics	$712.25	#87-214
acA4600-10uc - Basler	Basler	$712.25	#106538
Raspberry Pi 4 Model B - 4 GB RAM	AdaFruit	$55.00	#4296
32x32 RGB LED Matrix Panel - 4mm Pitch	AdaFruit	$29.95	#607
Pi Foundation Display - 7" Touchscreen Display for Raspberry Pi	AdaFruit	$79.95	#2718

APPENDIX G: GENT-IMERAJ_CV

- https://drive.google.com/file/d/1JZFlhp8M990J5n-lpiqWqK9tUY7rayzR/view?usp=sharing